

Superconducting Magnets for Particle Accelerators

Luca Bottura, Stephen A. Gourlay, *Senior Member, IEEE*, Akira Yamamoto, and Alexander V. Zlobin

Abstract—In this paper we summarize the evolution and contributions of superconducting magnets to particle accelerators as chronicled over the last 50 years of Particle Accelerator Conferences (PAC, NA-PAC and IPAC). We begin with an historical overview based primarily on PAC Proceedings augmented with references to key milestones in the development of superconducting magnets for particle accelerators. We then provide some illustrative examples of applications that have occurred over the past 50 years, focusing on those that have either been realized in practice or provided technical development for other projects, with discussion of possible future applications.

Index Terms—Superconducting, Magnet, Accelerator

I. INTRODUCTION AND HISTORICAL OVERVIEW

The phenomenon of superconductivity - vanishing electrical resistance in some metals at temperatures below 10 K - was discovered by Dutch physicist H. Kamerlingh-Onnes in 1911. However, it took more than 50 years to realize this phenomenon in practical superconducting magnets. Whether by chance or design, the first Particle Accelerator Conference (PAC) in 1965 coincided very closely with the first applications of superconductivity to particle accelerators. A search on the JACoW website yields 4 papers relating to superconducting accelerator magnets.

An interesting paper by Blewett [1] is almost as relevant today as it was then, especially this quote, “Of all the components in a circular high-energy particle accelerator, the magnet system, including the power supply, is predominantly the most expensive.” He mentions in the conclusions, the possibility of superconducting magnets for producing higher fields.

In the same inaugural PAC, held in Washington, DC, a paper by Fields and Laverick [2] discussed design considerations for superconducting magnets based on the demonstrated practicality of the recently successful superconducting ANL 67 kG, seven inch magnet system. Two of the predominant issues at the time were obtaining the maximum current in the conductor as determined by a measurement of a short sample and that the coils made from superconductors perform independent of any size or shape effects. This latter effect was related to the cable configuration and current sharing capability. A solution to these issues was

presented in a paper by Stekly and Zar [3] and led to further advances in superconducting magnet technology. The steady progress in the application of superconductivity to accelerator magnets is evidenced by the constant increase in PAC papers on the subject, Fig. 1. Initially the PAC conferences were held every two years and later joined by the European PAC and the Asian PAC. In 2010 the three conferences were merged into the International Particle Accelerator Conference (IPAC) and are held annually, rotating between regions. The original PAC has since become North American-PAC (NA-PAC) held every 18 months except when IPAC is held in North America.

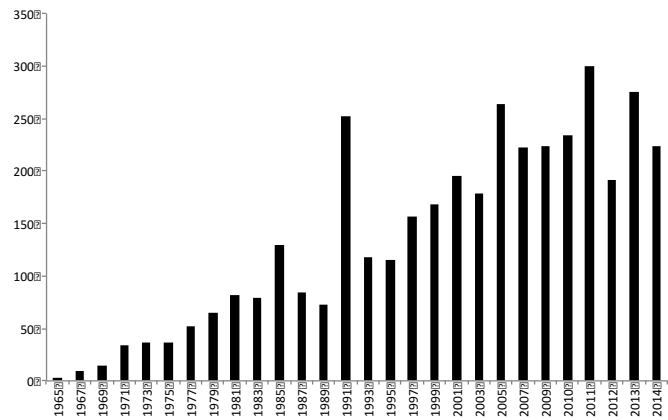


Fig. 1. PAC papers related to superconducting magnets for accelerators.

In the mid-60’s the superconductors of main interest were Nb-Zr, Nb-Ti and Nb₃Sn. Considerable focus was on designs of a 200 GeV accelerator and comparing superconducting with conventional magnets for the ring [4]. However, the challenges of superconducting accelerator magnets were still too great for implementation at this time and the earliest applications of superconductivity in high energy physics were for bubble chambers. [5]

The field took a significant step forward following the pivotal Brookhaven Summer Study in 1968 [6]. During this 6-week study, approximately 200 physicists and engineers from around the world came together to discuss the application of superconductivity for accelerators. The topics covered included,

This work was supported in part by the Director, Office of Science, High Energy Physics, US Department of Energy, under contract No. DE-AC02-05CH11231, and by Fermi Research Alliance, LLC, under contract No. DE-AC02-07CH11359 with the U.S. Department of Energy

L. Bottura is with CERN, TE-MS C M24500 CH-1211 Geneva 23, Switzerland (phone: +41-22-767-3729; email: Luca.Bottura@cern.ch).

S. A. Gourlay is with the Lawrence Berkeley National Laboratory, Berkeley, CA 94720, USA (phone: + 1 (510) 486-7156; email: sagourlay@lbl.gov).

A. Yamamoto, is with KEK and CERN, Tsukuba, 305-0801, Japan (phone: +81-28-879-6234; e-mail: akira.yamamoto@kek.jp).

A.V. Zlobin is with Fermi National Accelerator Laboratory, P.O. Box 500, Batavia, IL 60510, USA (phone: 630-840-8192; e-mail: zlobin@fnal.gov).

“Superconducting RF Cavities and Linacs,” “Cryogenics,” “Superconducting Materials,” “AC Effects” and “Flux Pumps.” The largest attendance for the program was on the topic of “Superconducting Magnets,” chaired by W.B. Sampson of Brookhaven and the final session covered “Accelerators and Storage Rings using Superconducting or Cryogenic Magnets.” At this time several high field alloys and compounds had been fabricated and in 1961, Kunzler at Bell Labs produced a 7.0 T field in a solenoid. This led quickly to higher field solenoids and a number of efforts to utilize the benefits of superconductivity for magnets were begun. However, the brittle nature of Nb₃Sn proved a difficult hurdle. Flexible tapes were developed to overcome the mechanical problem but proved vulnerable to flux jump instabilities, particularly in complex geometries required for accelerator magnets. Early forms of Nb-Ti wire also suffered from instabilities until multifilament Cu composite, twisted strands were developed in the 1968 – 1969 timeframe. This was a main topic of the Summer Study.

Several important topics were discussed in the magnet session. One that later proved to be one of the most important was the relationship between strand diameter and stability against flux jumps. Z.J.J. Steckly, and P.F. Smith of the Rutherford Laboratory discussed the advantages of fine filament superconductors in a conducting matrix that when twisted with an appropriately short length relative to the length of the wire would increase stability and reduce AC losses. Considerable discussion was directed toward the possibility of using superconducting beam handling magnets for the new 200 – 400 GeV accelerator being constructed at Weston, Illinois, originally the National Accelerator Laboratory and now known as Fermilab. Many of the papers presented at the 1969 PAC were based on proceedings of the BNL Summer Study.

At the 1971 PAC a panel discussion was held, briefly summarized by J.P. Blewett [7], that might be argued as the unofficial kick-off for superconducting magnets in accelerators. The panelists were geographically divided on two main issues: The European contingent did not want to consider the cost advantages of superconducting accelerators while the Americans argued a substantial cost savings and claimed that a 100 GeV superconducting synchrotron could be built in 5 or 6 years. The Europeans were more conservative and estimated 7 – 10 years. Work in the U.S. was concentrated in a few main centers: W.S. Gilbert presented the work at the Lawrence Radiation Laboratory in an overview of international efforts [8], R.R. Wilson mentioned the possibility of doubling the energy of the collider at NAL by post-acceleration with superconducting magnets, Brookhaven, represented by W.B. Sampson [9] was working on development of pulsed superconducting magnets and R. L. Martin represented the work at Argonne National Laboratory on furthering the development of superconducting magnets for accelerators [10].

In Europe, a consortium of three laboratories had been formed to prepare a program for future conversion of the recently approved 300 GeV accelerator to higher energy by using superconducting magnets. The membership of the organization, Group for European Synchrotron Studies (GESS), was Saclay, Rutherford laboratory and the Nuclear Research Center at

Karlsruhe. As an interesting note, there was a short paper referring to a “compacted fully transposed cable” produced at Rutherford Lab [11], giving a hint of what would be recognized as a transformational technology for superconducting magnets.

The tipping point had been reached and the 1970’s observed the launch of a large number of accelerator projects based on superconducting magnets and a growing R&D community. A new confidence in the collider approach based on the success of SPEAR at SLAC [12] and the Intersecting Storage Ring (ISR) at CERN along with the progress in superconducting technology led to ISABELLE at Brookhaven [13, 14], a 400 GeV proton collider, that was approved in 1977. The project suffered due to both scientific and political factors as well as problems with the 5 T superconducting magnets. Even though the problems with the magnets were overcome, the project was cancelled in 1983.

Other projects included the Fermilab Energy Doubler [15] and the Experimental Superconducting Accelerator Ring (ESCAR) at LBL [16] in the US, IR quadrupoles for the ISR at CERN [17], IR quadrupoles for TRISTAN at KEK [18] and UNK, an accelerator and storage ring complex in the USSR [19]. The UNK magnets were ambitious for the time, with a desired operating field of 5 T and 20% margin.

During this same time period, the cyclotron community was also moving toward the use of superconducting magnets with the usual advantage that higher fields lead to much more compact accelerators. A report issued by Chalk River Nuclear Laboratories in Ontario, Canada in 1974 [20] had an impact similar to the BNL Summer Study in jump-starting the move to superconductivity in cyclotrons. Groups from Michigan State University (MSU) and Chalk River, later joined by an Italian group, worked out many of the technical details. Due to political issues in both the US and Canada, MSU was awarded a grant in 1975 to construct a superconducting magnet and funding for the construction of a cyclotron at Chalk River was delayed until 1978. The MSU magnet, the heart of the K500 cyclotron, began operation in 1977 and beams were extracted in 1982 [21]. Superconducting cyclotron magnets were eventually constructed at Chalk River and Milan using pancake windings in contrast to the MSU choice of helical winding. The Milan magnet was eventually moved to Sicily for final construction of the cyclotron. In the following years, a K500 was built at Texas A&M and a K600 at Orsay/Groningen [22]. The construction of superconducting cyclotrons grew rapidly in the 1990’s [23], and the largest-scale superconducting cyclotron magnet system has been in operation as part of the RIKEN Superconducting Ring Cyclotron (SRC) system, including an associated superconducting radioisotope separator/beamline (named BigRISP), since the 2000’s [24, 25].

The technology matured and applications expanded into the 1980’s. HERA, an electron-proton collider, was getting underway at DESY in Germany [26]. ISABELLE was reborn as the Relativistic Heavy Ion Collider (RHIC) [27]. The Nuclotron, a fast cycling synchrotron, was under development at JINR (Dubna) [28]. There was considerable progress in conductor development as well. Nb-Ti was readily available from industry for construction of magnets with fields in the 5 T range and Nb-Ti-Ta and Nb₃Sn multi-filamentary conductors

were being pursued for fields up to 10 T. The first papers on the proposed Superconducting Super Collider (SSC) [29] were a dominant topic at the 1985 PAC and are responsible for the first peak in the publication distribution in Fig. 1. HERA began operation in 1992 while the SSC ramped up substantially and continued as the major source of PAC contributions. The large peak in 1991 was again due to the SSC and is easily explained - the PAC that year was held in Dallas, Texas, next to the site of the project. A summary of magnet progress is given in [30]. In that same year, the first papers on R&D for the Large Hadron Collider (LHC) at CERN were presented. A good overview of the project is given in [31]. The LHC soon became a ubiquitous topic at the PAC's. It currently represents the largest and most sophisticated use of superconducting magnets in an accelerator. The Nb-Ti, 8 T dipoles operate close to the practical limit of the conductor. The U.S. made a short-lived attempt to regain world leadership at the energy frontier by proposing a post-LHC hadron collider with a center-of-mass energy of 100 TeV, called the Very Large Hadron Collider (VLHC) [32]. Two versions of the collider were studied, a high field version using Nb₃Sn, cold bore magnets operating at 10 T, and a low field version, using combined function, transmission-line magnets with a warm bore [33]. Another concept to explore the energy frontier is a muon collider. The demands for superconducting magnets are extreme; collider ring magnets with the highest fields possible are desired, due to the short lifetime of the muon, and 40 – 50 T solenoids that are part of a complex cooling channel. This work has been a driver for applications of High Temperature Superconductors (HTS).

Heading into the next century the demands on superconducting magnet technology increased and broadened in scope. The Facility for Antiproton and Ion Research (FAIR) is an international accelerator facility under construction in Germany that will use antiprotons and ions to perform research in a broad range of physics and biological topics [34]. The original facility concept required a variety of superconducting magnets ranging from 2 T with a ramp rate of 4 T/s to 6 T at 1 T/s. The project has since been down-scoped by eliminating the 6 T magnet ring called SIS 300. In Japan, KEK was developing superconducting combined function magnets to transport a 50 GeV proton beam from the J-PARC facility for a neutrino experiment [35, 36]. As the LHC was moving forward, physicists focused their attention on the International Linear Collider (ILC), to complement the physics expected from the LHC. The collider was based on superconducting RF but the interaction regions required highly specialized magnets for the final focus [37].

Thanks to superconducting accelerator magnets, wound with strands and cables made of Cu/Nb-Ti composites, the energy reach of particle colliders has steadily increased. A view of this progress is shown in Fig. 2, in the form of a Livingston plot. The highest particle energies (reported as fixed target equivalent, in the laboratory frame) have been reached by proton-proton colliders. Since the Tevatron (1983) [38], through HERA (1991) [39], RHIC (2000) [40] and finally the LHC (2008) [41] all large-scale hadron colliders were built using superconducting magnets.

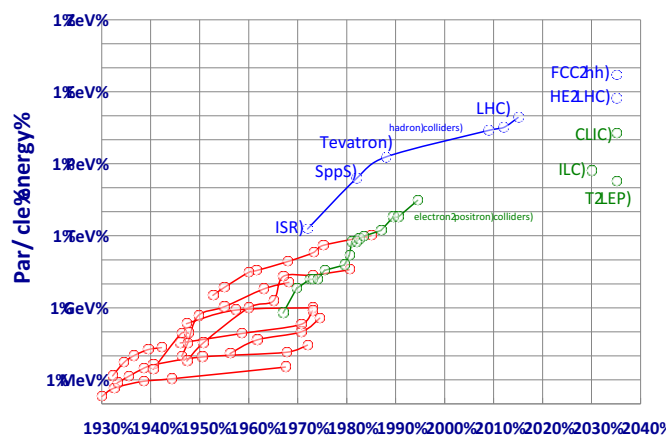


Fig. 2. Livingston plot of particle energy (in the laboratory reference frame, fixed target equivalent), where blue refers to hadron colliders and green to lepton colliders. Also shown are the proposed parameters for new colliders at the energy frontier

With the success of the LHC, the international high-energy physics community has again turned their attention to further exploration of the energy frontier. CERN is proposing a 100 TeV center-of-mass proton-proton collider called the Future Circular Collider (FCC) as the next step [42]. Focus is on a ring with a circumference of 80-100 km, necessitating superconducting magnets with operating fields from 16 to 20 T. This will be an unprecedented challenge for the magnet community, but one that they are eager to take on. In this paper we delve into a representative subset of applications of superconducting magnets for accelerators with an emphasis on the role of the Particle Accelerator Conferences. More comprehensive and detailed overviews can be found in [43], [44], [45].

The next section describes examples of superconducting arc and interaction region magnets for proton synchrotrons and storage rings. Section III, “Lepton Colliders,” reviews superconducting magnets used in present electron-positron circular machines as well as in the planned International Linear Collider and a future Muon Collider storage ring. The following sections IV and V, “Beam Lines” and “Some Special Magnets,” provide examples of superconducting magnet systems or magnetic elements used in modern particle accelerators.

II. HADRON ACCELERATORS/COLLIDERS

A. Arc Magnets

Accelerators for High Energy Physics (HEP) require large quantities of magnets, mainly dipoles and quadrupoles, whose function, in much simplified terms, is to guide and steer the particle beams, and confine them in a relatively small and well defined volume in the vacuum pipe. Magnets are also used to transfer beams from one accelerator into another, the transfer lines. Special magnet arrangements match beams from the transfer line into the injection insertions, or into ejection lines and beam dumps. They direct or separate beams for the RF cavities that accelerate the beams, shape it for the cleaning insertions, where collimators are located, and finally focus beams to collide at the interaction points where the experiments

reside. However, the function of the majority of the magnets is to keep the beam on a quasi-circular orbit. These are so called arc magnets, where dipoles and quadrupoles are placed periodically in a regular lattice that determines the longitudinal variation of the beam envelope. In the context of this paper we extend the definition of arc to the special region of the accelerator where the regular lattice is matched to the insertions and the beam functions are adapted, often referred to in large-scale HEP colliders as dispersion suppressor and matching sections.

In circular accelerators the bending (dipole) field of the arc eventually defines the final energy reach. In relativistic conditions, the relation between the beam energy, E (in TeV), the dipole field B (in Tesla) and the radius of the beam trajectory inside the bending field R (in km) takes a very simple form:

$$E \sim 0.3 B R \quad (1)$$

Equation (1) clearly shows the interest in high magnetic fields, namely to reach the highest possible energy for a given tunnel dimension, or to decrease the tunnel dimension (and the related cost) for a given energy. Indeed, Eq. (1) is the basic motivation for the extensive use of superconductors in colliders at the energy frontier, namely the possibility to generate fields largely in excess of the saturation limit for iron-dominated resistive magnets (up to 2 T) by flowing very large currents (of the order of 1 MA-turn) in a very limited space (a cross section of a few tens of cm^2) without the burden of resistive loss.

The main parameters of the largest superconducting hadron accelerators/colliders, and of their arc dipoles, are reported in Table I. The evolution of these parameters is very much related to the history of the development of the superconducting accelerator magnet technology, outlined below by making reference to the main innovations introduced in each of the colliders.

1) *The beginning: Tevatron*

As mentioned earlier, intense studies had led to the development of multifilamentary Nb-Zr, Nb-Ti and Nb₃Sn wires, awakening interest in superconducting technology, especially for experimental and detector magnets. It was however only later, in the early 70's, that the first prototypes of superconducting dipoles and quadrupoles demonstrated that superconducting magnet technology could bear significant interest for accelerator applications. These were mainly the fruit of the pioneering work at the Rutherford Laboratory and at BNL [6]. Superconducting magnet technology was one of the initial options for the construction of the new CERN accelerator, the SPS, rapidly discarded in favor of resistive magnets. This was not the case at the Fermi National Laboratory, where in the same years R. R. Wilson was pursuing a project to upgrade the Main Ring beyond 500 GeV. The project was initially presented as an Energy Doubler, but rapidly became known by the very modern name of Energy Saver, and is now known as the Tevatron collider for protons and anti-protons. The Tevatron arc magnets were the result of years of intense and extremely effective R&D.

TABLE I.
CHARACTERISTICS OF MAJOR SUPERCONDUCTING HADRON ACCELERATORS
AND DETAILS FOR THE ARC DIPOLES

	Tevatron [38]	HERA [39]	RHIC [40]	LHC [41]
First beam	7-1983	4-1991	6-2000	9-2008
Maximum beam energy (GeV)	980	920 [#]	250* 100/n**	7000
Injection energy (GeV)	151	45	12	450
Ring length (km)	6.3	6.3	3.8	26.7
Number of main dipoles	776	416	264	1232
Configuration	Single bore One SC ring	Single bore One SC ring	Single bore Two SC rings	Twin bore One SC ring
Dipole magnetic length (m)	6.1	8.8	9.45	14.3
Aperture (mm)	76	75	80	56
Dipole field (T)	4.3	5.3	3.5	8.3
Operating temperature (K)	4.6	4.5	4.3-4.6	1.9
Operating current (kA)	4.3	5.7	5.1	11.9
Current ramp-rate (A/s)	56	43	80	10
Stored energy (MJ)	0.30	0.94	0.35	6.93
Coil geometry	Double layer	Double layer 4 blocks	Single layer 4 blocks	Double layer 6 blocks graded
Number of turns	35/21	32/20	31	15/25
SC strand		Nb-Ti		
Strand diameter (mm)	0.68	0.84	0.65	1.065/0.825†
SC filament diameter (μm)	9	14	6	7/6†
Cu:SC ratio (-)	1.8	1.8	2.25	1.65/1.95†
Strands in cable	23	24	30	28/36†
Cable dimensions (H mm x W mm)	1.26x7.77	1.48x10	1.16x9.7	1.9x15.1 1.48x15.1†

(#) Energy of the proton beam, colliding with the 27.5 GeV electron beam

(*) Particle energy for proton beams

(**) Particle energy per nucleon, for ion beams (Au)

(†) Inner/Outer layer grade cable

The rise of the application of superconductivity for accelerators was triggered by the success of the Tevatron. It contained 776, 6.1 m long superconducting dipoles connected in series in a 6.3 km cryogenic ring, operating at 4.6 K. The arc dipole magnets of the Tevatron could reach a flat-top field of 4.3 T, with a relatively fast ramp, of the order of 100 mT/s, and would operate at the flat top for hours of physics, an ideal working mode for superconducting magnets. Hosting two beams in the same pipe, the magnets required a relatively large aperture, 76 mm. A cross section of the arc dipole is shown in Fig. 3.

The Tevatron magnets were based on Rutherford cable, used for the first time in a full-scale magnet, which has become standard practice since. A Rutherford cable, one example shown in Fig. 4, is composed of fully transposed Cu/Nb-Ti twisted wires. The rectangular geometry of the cable provides a high packing factor, and results in the precisely controlled dimensions (few μm) that are necessary to wind coils of accurate geometry (typically 20 μm), and is flexible enough to accommodate various geometries. A short strand transposition

length limits coupling loss and ensures good current distribution, also aided by the electrical contact between the strands. In the case of the Tevatron, the 23 strands in the cable were coated to control the eddy currents induced during ramps. The configuration chosen, with 12 strands coated with dark Ebanol, and 11 strands coated with shiny Stabrite, made a familiar striped pattern, hence the nickname “Zebra” cable [46].

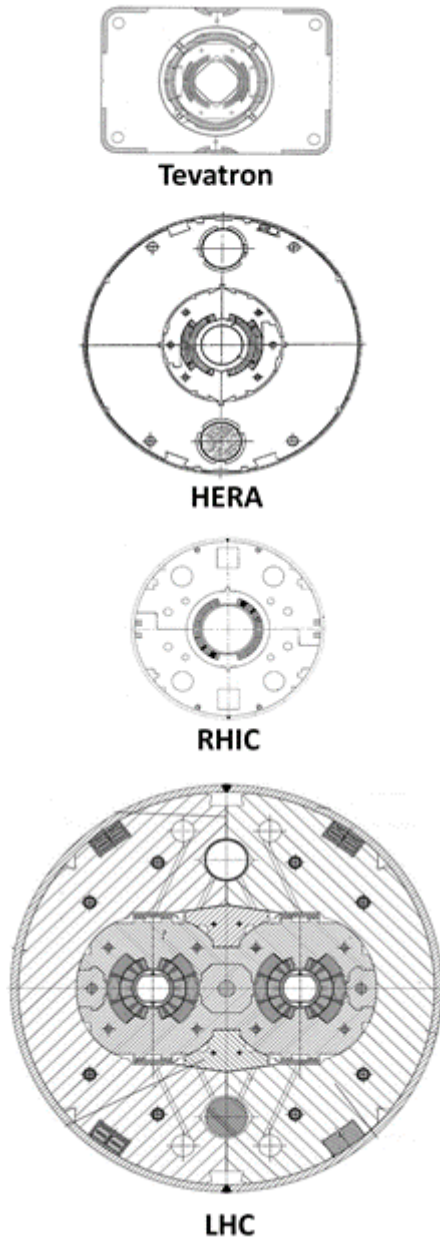


Fig. 3. Cross section (to scale) of the dipoles of the four major superconducting hadron accelerators built to date.

The strand, the basic building block, was another major innovation. Fermilab supplied raw materials (the Fermi-kit) to the manufacturers in an attempt to achieve homogeneous performance, reduce cost and foster competition. The program resulted in the first large-scale production of Nb-Ti strand and largely contributed to the creation of the modern MRI market [47].

The second major breakthrough in the Tevatron dipoles was the use of a system of *collars* to react the electromagnetic force and to apply an initial pre-stress to the coil in order to avoid movement due to Lorentz forces that would lead to heat generation, driving the conductor normal. The coil in the collar can be pictured as a *roman arch*, where the pre-compression is achieved by inserting an oversized wedge into the coil pole. The collars, assembled in halves around the coil and locked by keys, provide the radial load that translates into the required coil pre-compression.

Finally, trying to keep the cold mass as small as possible, the decision for the Tevatron design was to use a cold coil in a warm iron yoke. This resulted in centering and alignment issues, as the fiducial references had to follow thermal contractions. This problem was solved by the use of spring-loaded smart-bolts. All in all, the design of the Tevatron dipoles paved the way to the development of the following accelerators.

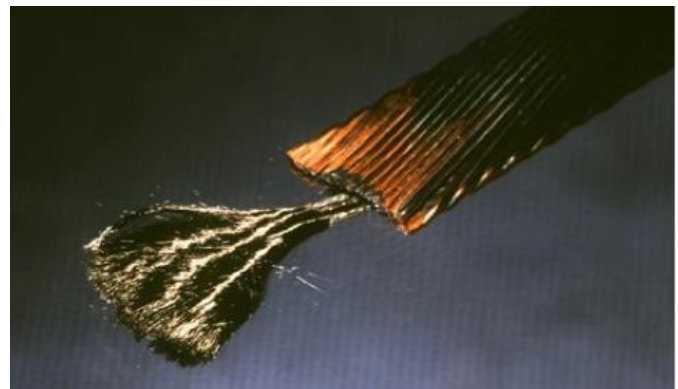


Fig. 4. A Rutherford cable for the inner layer of the LHC dipoles, showing the Nb-Ti filaments in a few etched strands.

2) Adolescence: HERA and RHIC

While the Tevatron was in construction, the DESY laboratory in Hamburg was designing an electron-proton collider ring, HERA. The arc dipoles of the HERA proton ring had an aperture and field similar to the ones at the Tevatron, 75 mm and 5 T respectively, as well as similar accelerator dimensions, 416 magnets of 9.8 m length over a total perimeter of 6.3 km. The HERA dipoles, whose cross section is shown in Fig. 3, mainly differed from those at the Tevatron because of the use of a cold iron yoke, and an outer shell that provided helium leak tightness. A cold iron concept had been developed earlier at ISABELLE [14], the initial competitor of the Tevatron. This concept greatly simplified the alignment and geometry of the coil, at the expense of a much larger cold mass but had to accommodate the differential thermal contraction between the outer stainless-steel shell, the iron yoke, the aluminum collars and the composite copper/Nb-Ti/insulation coil. The HERA arc magnets were manufactured in industry, which required a significant escalation in the understanding and control of the technology.

The operation of the HERA proton ring was greatly influenced by persistent currents, the residual field due to the diamagnetic moment of the superconducting filaments. The use of a relatively large filament diameter in the HERA Nb-Ti strands (of the order of 14 to 16 μm) resulted in good critical

current, but posed challenges in performance. Understanding of this phenomenon in a running accelerator drove the push towards fine filaments.

A few years later, and following the closure of the SSC, the tunnel originally planned to host ISABELLE at BNL was used for the installation of the Relativistic Heavy Ion Collider (RHIC). RHIC is an ion-ion collider consisting of two independent rings of 3.8 km length. The arc dipoles have a large aperture of 80 mm, and produce a modest nominal field of 3.5 T, see Fig. 3. The main focus for the RHIC magnets was to achieve a low specific cost, which translated in the use of a single-layer and thin coil design, and an iron yoke very close to the coil, producing approximately 30 % of the total field in the bore. The coil was wound using high performance Nb-Ti conductor developed in a program for the Superconducting Super Collider (SSC) [48]. The critical current density (J_c) was in excess of 2700 A/mm² at 4.2 K and 5 T with 5 to 6 μ m filaments. Glass-filled phenolic spacers were substituted for the metallic collars that had been used for the Tevatron and HERA.

Coil pre-stress was applied directly by welding the outer He-containment shell, across the split iron yoke, through the spacers. As for HERA, the production of the RHIC dipoles took place in industry, and was assisted by systematic measurement of the geometric field harmonics as a tool to decide on corrective actions.

3) *Maturity: the LHC*

The concept of a Large Hadron Collider (LHC) at CERN arose in the mid 80's, and started with a relatively low-profile R&D program. The initial concepts were very much based on the large endeavor on-going at the US-based SSC. To be competitive with the SSC, the LHC had to push Nb-Ti magnet technology to the highest reasonable field. This was possible by

- Drawing on the concepts proven in previous accelerators, and specifically the use of collars and a cold iron yoke;
- Taking stock of the two-in-one design that had been proposed, and abandoned, as a part of the ISABELLE study (then renamed the Colliding Beam Accelerator, CBA) and SSC;
- Profiting from the recent understanding and development of Nb-Ti, that had increased the current density by nearly a factor 2 thanks to the use of high-homogeneity Nb-Ti alloy [48];
- Applying superfluid (1.9 K) cooling on a large scale for maximizing Nb-Ti conductor performance and the magnet operating field.

The result of this process is shown in Fig. 3, the twin aperture LHC dipole, where the two beam pipes are mechanically coupled in a single collared coil assembly. This required careful optimization at the level of the magnetic design and production follow-up to insure that both apertures had the same integrated field, with little coupling quadrupole generated in one aperture by the return field of the other aperture. Cooling to 1.9 K increased the field reach of Nb-Ti by approximately 3 T, resulting in a nominal operating field of 8.33 T in an aperture of 56 mm. Finally, with a relatively small aperture and a coil very

close to the beam, field quality was extremely important. The LHC strands have a filament diameter in the range of 6 to 7 μ m, to limit persistent currents. An effective procedure of Sn-Ag coating and oxidation was developed to control the inter-strand resistance to values above a minimum of 10 $\mu\Omega$ (to limit coupling currents) and below a maximum of 200 $\mu\Omega$ (to allow current redistribution).

4) *Rebirth: the HL-LHC upgrade and the Future Colliders*

The results from the coming run-II of the LHC, in the years 2015 - 2018, will be critical to provide leading directions for HEP in the future. It is nonetheless very likely that the path towards higher luminosity and particle energy, and the associated increase of discovery potential, will continue.

The first, and immediate example is the High-Luminosity LHC (HL-LHC) project, whose main objective is to increase the LHC luminosity at the ATLAS and CMS experiments by a factor of five. This requires very large aperture interaction region (IR) quadrupoles, with field levels at the coil in the range of 12 T [49], described later in this article. In addition, the need for additional collimators in the LHC will be satisfied with arc dipoles of shorter length and increased bore field, of approximately 11 T [50].

A second example is the search for physics beyond the Standard Model, corresponding to the proposed future colliders shown in Fig. 2. These proposed accelerators respond to the recommendation of the European Strategy Group for Particle Physics [51], calling for a study of an accelerator that should follow the LHC at the energy frontier. Among the possible responses is the design study of a Future Circular Collider (FCC) for hadrons with energy of 50 TeV per beam, a 7-fold increase with respect to the nominal LHC conditions. A first analysis of the general parameters for such a machine has led to a baseline configuration requiring 16 T dipoles in a tunnel of approximately 100 km in length. An initial siting study also pointed to a possible variant with reduced tunnel diameter, and 80 km length [52]. This variant, which would require 20 T dipoles to reach 50 TeV per beam, is presently considered as an option in the scope of the FCC design study.

The FCC design study is the natural sequel to the initial considerations on the possibility of an energy upgrade in the LHC tunnel, i.e. a High Energy LHC (or HE-LHC) that could provide a proton energy of 16.5 TeV per beam [53], [54] by using 20 T dipoles, i.e. the same as specified for the 80 km FCC option. Configurations and performance similar to those in the scope of the FCC design study are taken as a baseline for a similar study of a 54 km length, double-purpose lepton and hadron collider proposed in China, under the auspices of the Institute of High Energy Physics (IHEP) in Beijing. The tunnel would host in this case an electron positron machine (Circular Electron Positron Collider, CEPC) followed later with installation of 20 T magnets for a proton-proton collider (Super proton-proton Collider, SppC) with a center of mass energy of 70 TeV range [55].

The palette of HEP is however not confined to hadron machines. Among the alternatives that have been considered, it is important to mention the Muon Accelerator Program (MAP)

that produced a roadmap that would lead to a muon collider with a high-intensity neutrino factory as the first stage [56], [57]. A muon collider in the range of 1.5 to 3 TeV center of mass energy would have a modest dimension, 2 km diameter, but would require arc magnets with bending fields in the range of 10 to 14 T, very high field capture solenoids, from a minimum of 20 T up to 50 T, and large aperture IR magnets, possibly with an open mid-plane, to tolerate the high radiation loads.

The HL-LHC project, the HE-LHC study, the FCC design study, the MAP and its intermediate steps, are all strong drivers for the development of superconducting magnets producing accelerator quality bore fields beyond those produced by the LHC dipoles. This immediately calls for superconducting material, or a combination of materials, with critical field and critical current higher than Nb-Ti. In practice, Nb₃Sn is the prime candidate to develop accelerator magnets beyond 10 T.

5) Magnets for rapid cycled synchrotrons

High fields are not always the primary goal for collider magnets. High ramp rates at lower fields are sometimes required for a particular application. Although the ideal operating mode for superconducting magnets is steady state, considerations of operating cost have also driven a growing interest for their use in the case of large installations, such as the Nuclotron (in operation since 1994) at the Joint Institute for Nuclear Research (JINR, Russia) [58] and the Facility for Antiproton and Ion Research (FAIR) under construction at GSI in Darmstadt (DE) [59]. The main challenge for fast cycled accelerator magnets is to achieve the desired field at the specified repetition rate, economically and reliably. This requires special attention to AC loss and cooling, and to maintain the required operating margin by removing the heat generated during ramping. In addition, reducing AC loss is mandatory to achieve favorable economics (the cryo-plant investment and operation costs are major drivers). Quench detection and protection is demanding as the coils are powered at relatively high voltage, and the reliable discrimination of a resistive signal that can be smaller than 0.1 % of the inductive voltage becomes a challenge. Eddy currents, and means to reduce them, need to be included in the design from the start. Finally, cycling several 10⁸ times, material fatigue is important.

The Nuclotron in operation since 1994 at JINR is a fast cycling superconducting ring with a circumference of ~0.25 km. It consists of 96 dipoles, 64 quadrupoles and 32 correctors. The design of the main magnets is based on a superferric window-frame concept where the magnetic field is formed by a cold iron yoke. The magnet coils are wound using a hollow cable cooled by circulating two-phase liquid helium at 4.5 - 4.7 K. The vapor content varies from 0% at the magnet inlet to 90% at the outlet. The cable consists of a twisted layer of Nb-Ti strands on a 5 mm diameter Cu-Ni pipe. Thanks to the low inductance and efficient coil cooling, the magnets can operate in fast cycling modes up to 2.2 T with a field ramp rate up to 4 T/s. The magnets are surrounded with thermal shields and suspended inside the vacuum vessels using stainless steel rods. The Nuclotron dipole and superconducting cable are shown in Fig. 5.

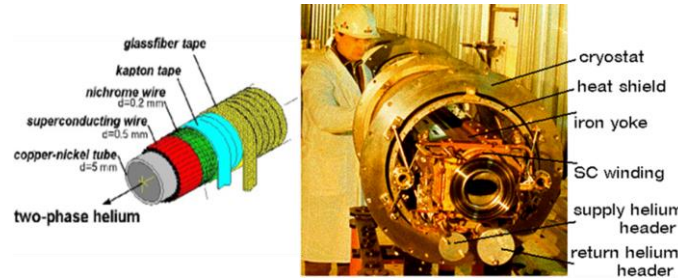


Fig. 5. Schematic view of the superconducting cable (left) and the Nuclotron dipole in cryostat (right).

FAIR will be an accelerator complex consisting of a main synchrotron, the SIS-100, with a magnetic rigidity of $B\rho = 100$ T-m, feeding a number of transfer lines, separators (and in particular the superconducting SFRS), spectrometers and storage rings (CR, RESR, NESR, HESR) hosting experiments mainly dedicated to nuclear physics. Among the large variety of magnets, the most challenging one is possibly the dipole for the SIS-100. To achieve the desired rigidity, the SIS-100 dipole has a bore field of 2 T, and requires a nominal cycle time of 1 s, i.e. approximately 4 T/s ramp-rate. The magnet is superferric, with a window-frame, cold iron yoke and saddle coils wound as a single block. A prototype of the SIS-100 dipole is shown in Fig. 6, where the rectangular bore of 130 mm \times 65 mm is clearly visible. This design is largely inspired by the Nuclotron.

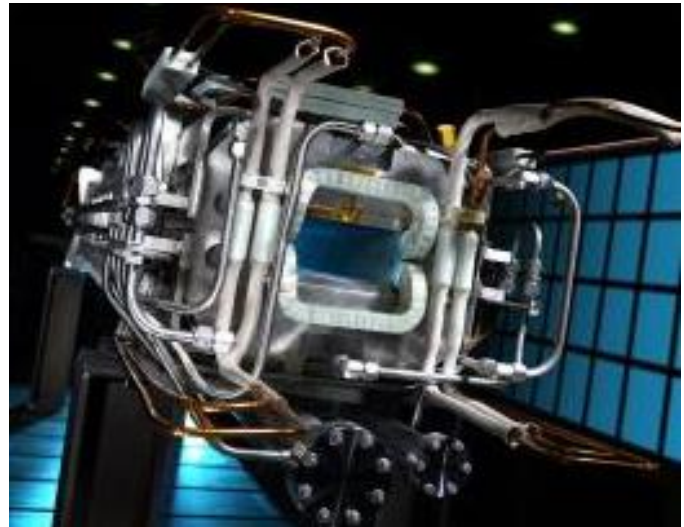


Fig. 6. Prototype SIS-100 dipole, by courtesy of BNG (Germany).

One of the options considered initially in the FAIR complex, and presently existing only as magnet R&D, was to complete the accelerator chain with a higher energy synchrotron SIS-300, with $B\rho = 300$ T-m. The dipoles of SIS-300 require a higher field, 4.5 T, in a 100 mm bore, and would be ramped at 0.5 to 1 T/s. This magnet is still at the design and model stage, but the baseline design uses a cos θ coil layout. Design and model magnets have been produced in a collaboration between GSI/FAIR, and BNL in the USA [60], and since 2006 with INFN in Italy [61]. The latest design features a curved coil with a relatively large sagitta of 28 mm over a 4 m length. The magnet

cross-section, and the first coil produced showing the large degree of curvature, are shown in Fig. 7

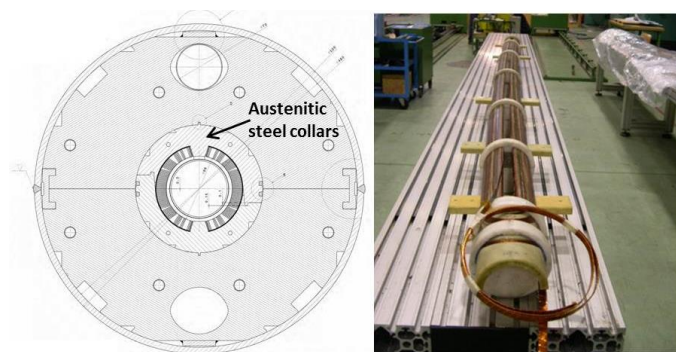


Fig. 7. Cold mass cross section (left) of the SIS-300 dipole, and a photograph of the first coil (right) by courtesy of ASG (Italy) after INFN.

B. Magnets for Interaction Regions

In particle accelerators beams are brought into collision using interaction region (IR) magnets. The quantity that measures the ability of a particle accelerator to produce the required number of interactions is called the *luminosity* and is the proportionality factor between the number of collisions per second and the production cross section. With higher luminosity the probability of detecting new particles increases, creating opportunities for new physics discoveries. The luminosity is approximately inversely proportional to the area of the colliding beams at the interaction point (IP). The transverse beam size can be reduced at the collision point by using stronger final focus quadrupoles.

IR magnets include high field dipoles for beam steering (separation and recombination) as well as high gradient quadrupoles for beam focusing. Depending on the order of these magnets with respect to the IP, the IR design is referred to as a “dipole first” or a “quadrupole first” layout. The requirements and operating conditions in the vicinity of the interaction point make the design and parameters of these magnets more stringent than for arc magnets. The most important requirements for insertion magnets include [62], [63]:

- High gradient/field to achieve the required β^* and beam separation/recombination within a limited insertion space.
- Large aperture to house beam dynamic apertures to meet the β^* requirement, transverse beam separation due to the crossing angle and radiation/heat deposition absorbers.
- Good field quality in large aperture due to large beam sizes inside the low-beta insertions as well as beam crossing angle resulting the beam separation in the single IR quadrupole aperture.
- High radiation tolerance and thermal stability to withstand high radiation load on insertion magnets.
- Alignment and mechanical stability to maximize luminosity, physical and dynamic apertures.

High field and aperture lead to large stored energy and Lorentz forces in IR magnets complicating quench protection and mechanical structure. A high radiation environment and

associated heat deposition requires a design that minimizes exposure to radiation, use of radiation resistant materials, and providing adequate temperature margin and coil cooling.

The IR magnets used in the Tevatron, HERA, RHIC, and LHC, are summarized in Table II. All the magnets utilize Rutherford cables with Nb-Ti strands. IR magnets for future accelerators will require the higher performance Nb₃Sn and HTS materials. The LHC luminosity upgrade is an excellent opportunity to use Nb₃Sn technology. This experience, including magnet production and operation in a real machine, will be of critical value in designing magnets for the Future Circular Collider (FCC).

TABLE II.
PARAMETERS OF SUPERCONDUCTING IR QUADRUPOLES

Parameter	ISR	Tevatron	RHIC	LHC
G_{nom} (T/m)	42.7	140	48.1	215
Coil ID (mm)	173*	70.2	130	70

* Warm bore

1) ISR insertion quadrupoles

The CERN Intersecting Storage Rings (ISR) complex, proposed in 1963, was the first proton–proton collider. It was operational from 1971 to 1984, demonstrating both the great potential of colliding-beam physics and the vigorous progress in accelerator physics and technology. The ISR consisted of two proton synchrotrons 300 m in diameter intersecting in eight interaction points with 15 degree crossing angles. The first low- β insertion at one particular interaction point using conventional quadrupoles was completed in 1974. Then more powerful focusing insertions based on superconducting quadrupoles were proposed. After successful construction and operation of a superconducting quadrupole prototype [64] the construction of a complete high-luminosity insertion was approved in 1977 [17]. In July 1978 it was decided to install an insertion at intersection I8 with a large axial magnetic field spectrometer. Besides its importance for physics, it was the first attempt to use superconducting magnets in an operating storage ring. Moreover, the construction of 8 superconducting quadrupoles to tight specifications was done by industry, which was also a significant technical challenge.

Fig. 8 (bottom) shows a longitudinal cross section of an ISR IR magnet. The conductor of the main coils was a solid composite wire of rectangular cross-section 1.8 mm by 3.6 mm, containing about 1250 twisted 50 μm diameter Nb-Ti filaments inside a copper matrix, and insulated with enamel and polyimide tape. Each coil had 290 turns, wound in three blocks on a central stainless steel post with copper wedges to approximate a $\cos 2\theta$ current distribution. A section of the coil is shown in Fig. 8 (top). The coil ends had a constant perimeter profile to ease winding under tension. Each coil was individually vacuum-impregnated with epoxy resin.

The four coils were wrapped together with glass-epoxy bands, to form a compact self-supporting cylinder, that could withstand the pre-compression applied by the steel quadrants when the aluminum rings shrink at cool-down. An optimal preload prevented deformation under Lorentz forces. Two full-scale prototypes operated repeatedly and reproducibly at a gradient of

45 T/m with a current of 1680 A that corresponds to a maximum field of 5.8 T. The magnets did not show any retraining after repeated warm-up and cool-down. When pulsed up to quench, the magnets were able to absorb their stored energy of 700 kJ without damage.

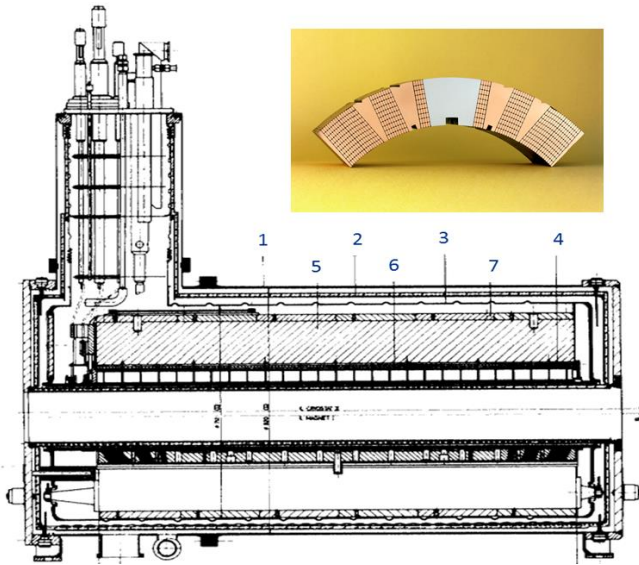


Fig. 8. Quadrupole coil cross-section (top right) and longitudinal cross-section of an ISR IR magnet in the cryostat (bottom): 1 - vacuum vessel; 2 - radiation screen with superinsulation; 3 - helium vessel; 4 - stainless steel spacer; 5 - iron yoke; 6 - coil bandage; 7 - shrinking rings. Photo provided courtesy of CERN. (CERN-PHOTO-7808567X)

The sextupole coils were wound using solid rectangular enameled conductor of 1.3 mm by 0.7 mm. They produced a sextupole component of 24.1 T/m at 220 A. The sextupole coils as well as the dodecapole correction coils were placed in grooves in the wall of the helium vessel inner tube and pre-compressed by means of epoxy silica wedges wrapped by aluminum-alloy wire under tension. The magnet helium vessel was suspended in the cryostat by Inconel bands attached to the ends. The magnet was cooled by natural convection in nucleate boiling helium at 4.3 - 4.4 K.

2) Tevatron insertion quadrupoles:

In the middle of 1980's Fermilab developed and successfully operated low-beta insertions with superconducting quadrupoles in the Tevatron D0/B0 interaction regions [65], [66], [67]. Each low-beta insertion consists of 18 quadrupoles powered as 11 independent circuits to reduce the β^* to 25 cm, where β^* is related to the transverse beam size. Low beta is reached with a set of 140 T/m quadrupoles. Weaker 70 T/m quadrupoles match the low-beta insertion to the rest of the accelerator lattice. Since the protons and antiprotons share the same aperture in Tevatron magnets, separation of the two beams everywhere except at the desired collision points is provided by electrostatic separators placed in the lattice gaps.

A cross-section of the 140 T/m quadrupole is shown in Fig. 9. The magnet has a two-layer coil and a cold iron yoke. The coil inner diameter is 70.2 mm. The coils are wound using Rutherford cable with 36 Nb-Ti strands each 0.628 mm in diameter. Each pole contains 19 inner and 28 outer turns. The coils are clamped with aluminum collars supported by a 170 mm

inner diameter and 48.5 mm thick iron yoke and a stainless steel shell. The cold mass is surrounded by a two-phase helium channel, a liquid nitrogen shield and a square vacuum vessel. Special posts support the cold mass and thermal shields inside the vacuum vessel. The magnetic length of the quadrupoles varies from 606.4 to 5892.8 mm.

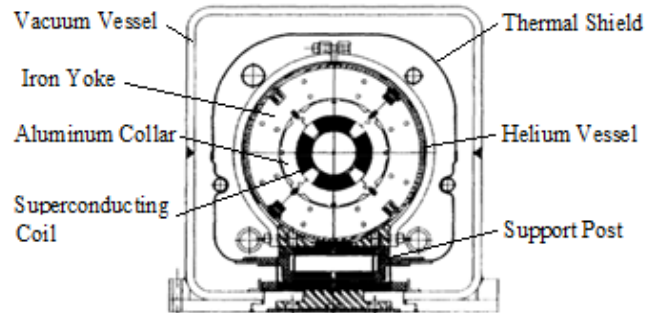


Fig. 9. 2-layer Tevatron IR quadrupole.

A cross-section of the 70 T/m quadrupole is shown in Fig. 10. The quadrupole has a single-layer coil and a cold iron yoke. The coil inner diameter is 70.2 mm, the same as the two-layer coil. To reduce the operating current and the heat leak through the current leads, the coil was wound with flat cable made of 5 parallel, insulated Nb-Ti strands. Each pole has 13 turns. The bare strand sizes are 1.09 mm and 1.76 mm. The magnet cold mass has an outer diameter of 190.5 mm and a physical length of 762 mm with a magnetic length of 546.1 mm. These magnets replaced some correctors in existing multipole corrector components.

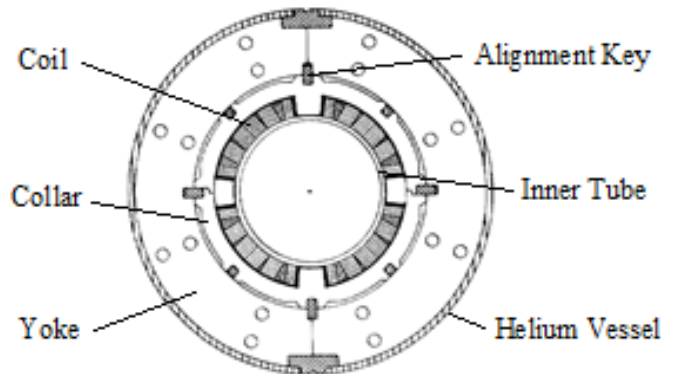


Fig. 10. Single-layer Tevatron IR quadrupole.

3) RHIC insertion magnets:

Interaction insertions in RHIC use a dipole first layout. In this layout the separation DX and recombination D0 dipoles are placed between the IP and the final focus triplets Q1-Q3 [40].

The 130 mm final focus quadrupoles Q1-Q3 [68] are arranged in a triplet configuration and installed on each side of the interaction point. Since the two colliding beams do not share a common aperture, each beam passes through independent triplets. The inner triplets and the adjoining D0 bending magnets from both rings are installed inside a common vacuum tank in situ. Similar to the arc quadrupoles these magnets use single-

layer coils but are made of a Rutherford cable with 36 Nb-Ti 0.648 mm diameter strands, phenolic coil-yoke spacers, and a cold iron yoke. A cross-section of the 130-mm quadrupole cold mass is shown in Fig. 11.

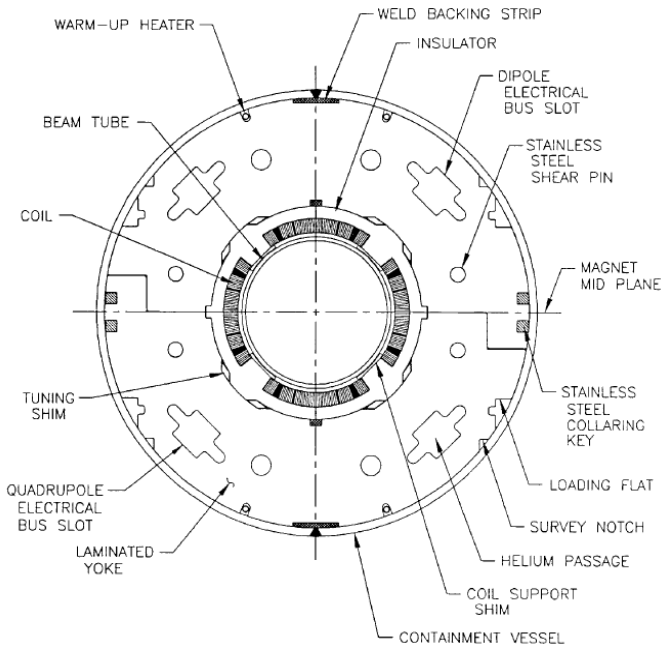


Fig.11. Cross-section of the RHIC IR quadrupole.

Each quadrupole coil has 27 turns and two copper wedges to control field quality. The iron yoke OD is 350.5 mm. It has holes for electrical buses, helium, and iron saturation control. The quadrupole along with correctors is placed inside a helium vessel formed by a stainless steel skin. The Q1-Q3 nominal gradient is 48.1 T/m at 5.05 kA. The magnetic lengths of Q1, Q2 and Q3 are 1.44, 3.40 and 2.10 m respectively.

100 mm recombination dipoles D0 [69] guide the beams into collision at the interaction point. The D0 nominal field is 3.52 T at 5 kA and the magnetic length is 3600 mm. Although each dipole contains a single beam, the larger aperture is required to accommodate the large beam size in the low-beta insertion, the beam crossing angles, and also collisions between different particles. The D0 mechanical design is similar to the arc dipole. The two D0 magnets on the same side of the IP are placed in a common vacuum vessel. This limits the outer diameter of the D0 yoke to 310 mm. A cross-section of the D0 cold mass is shown in Fig. 12.

The D0 cable has 30 Nb-Ti 0.648 mm diameter strands, the same as the cable in the arc dipoles. To achieve the required field quality at injection, a single-layer, five-block coil design was used. It has four wedges and 40 turns per half-coil. Due to the limit on the yoke radial size, the coil aperture was restricted to 100 mm. The magnet also has a mechanical sagitta of 7.6 mm. To simplify interconnections, D0 dipoles with opposite curvatures were used.

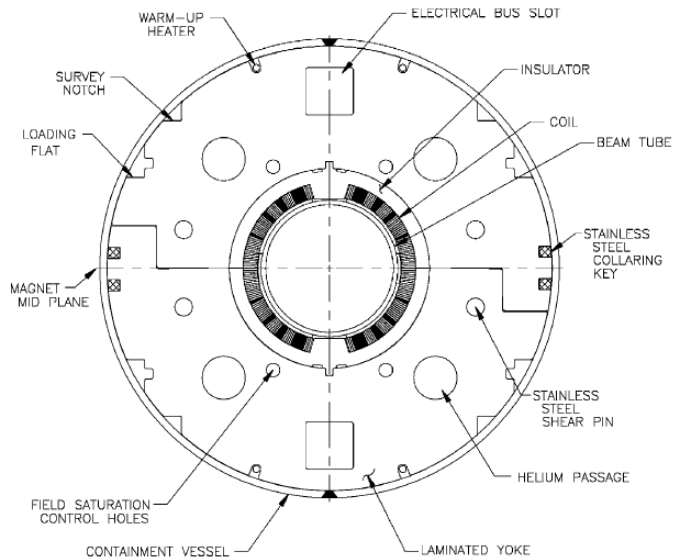


Fig.12. Cross-section of the RHIC recombination dipole (D0).

The 180 mm separation dipoles DX [70] are located directly on either side of the interaction points. Both beams pass through the magnet aperture. The magnet strength controls the collision angle. The two-beam separation and the field quality at the magnet far end determine the magnet aperture of 180 mm. The limited axial space in the lattice requires a nominal field of 4.3 T at 6.6 kA that is higher than in the arc dipoles. To achieve this field with a sufficient margin, a wider cable was used. The DX magnetic length is 3700 mm. Fig. 13 shows a cross-section of the DX cold mass.

The single-layer 6-block coil has 70 turns of Rutherford cable with 36 Nb-Ti 0.648 mm diameter strands. This magnet uses 40.1 mm wide stainless steel collars, and a cold iron yoke with an outer diameter of 622 mm. Iron saturation is controlled by holes in the yoke including the 31.75 mm diameter helium channels. Quench protection heaters and a diode across each of the two coils were used to protect the magnets during a quench.

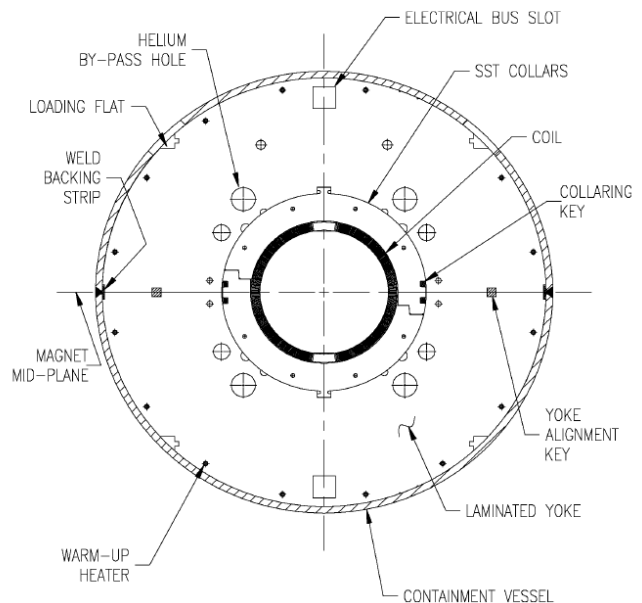


Fig.13. Cross-section of the RHIC separation dipole (DX).

4) LHC IR quadrupoles

LHC IRs use large-aperture inner triplets followed by single-aperture separation dipoles D1, and twin-aperture recombination dipoles, D2. The beams are separated by 1.28 T normal conducting dipoles. The D1 dipoles consist of six 3.4 m long 60 mm aperture modules. The recombination dipoles, D2, are Nb-Ti magnets with 10 mm thick single-layer RHIC-type coils of 80 mm aperture [71].

The present LHC low- β triplet is composed of four Nb-Ti quadrupoles Q1, Q2a, Q2b and Q3 with a coil aperture of 70 mm [72]. The magnets are cooled with superfluid helium at 1.9 K using a heat exchanger capable of extracting up to 10 W/m. Two types of quadrupoles are used in the triplet: 6.6 m long MQXA magnets developed by KEK, and 5.7 m long MQXB magnets developed by Fermilab. The MQXA magnets are used as Q1 and Q3 quadrupoles, while the two MQXB's are used as the Q2a and Q2b quadrupoles. The magnetic length of Q1 and Q3 is 6.37 m. The magnetic length of the Q2's is 5.5 m.

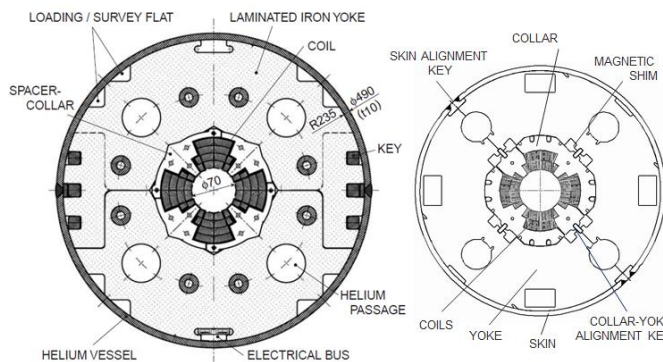


Fig. 14. LHC IR quadrupoles: MQXA (left) and MQXB (right).

The high-gradient, large-aperture low- β quadrupoles are the most demanding magnets in the LHC. They must operate reliably at 215 T/m, provide excellent field quality, and sustain high heat loads generated by secondary particles emanating from beam collisions. The MQXA and MQXB cross-sections are shown in Fig. 14.

The MQXA quadrupole design is based on a four-layer coil made of two 11 mm wide Nb-Ti Rutherford cables [73], [74], [75]. The inner cable has 27 strands, 0.815 mm in diameter. The outer cable has 30 strands, 0.735 mm in diameter. The coils are fabricated in two separate double layers and are assembled using spacer-type stainless steel collars. The coil pre-stress and radial support are provided by the cold iron yoke, which consists of horizontally split laminations keyed at the mid-plane.

The MQXB design features a two-layer coil, with each layer individually wound using a 15.4 mm wide Rutherford-type graded Nb-Ti cable [76]. The inner cable has 38 strands, 0.808 mm in diameter. The outer cable has 46 strands, 0.648 mm in diameter. The coils are assembled using free-standing stainless steel collars, which provide the pre-stress and balance the magnetic forces. The collared coil assembly is aligned in the iron yoke with alignment keys and the magnet is enclosed in a stainless steel helium vessel consisting of half-shells welded at the pole plane. The MQXA and MQXB parameters are compared in Table III.

TABLE III.
MQXA AND MQXB IR QUADRUPOLE PARAMETERS.

Parameter	MQXA	MQXB
Coil aperture (mm)	70	70
Yoke OD (mm)	470	400
G_{nom} (T/m)	215	215
I_{nom} (A)	7149	11950
Magnetic length (m)	6.37	5.5
Stored energy (MJ)	2.3	1.36

The LHC IR quadrupoles have essentially reached the limit of Nb-Ti technology. The maximum field in the coil under operating conditions exceeds 8 T, and the conductor limit approaches 10 T. They require cooling by superfluid helium at 1.9 K to achieve the nominal field gradients needed by LHC.

5) IR magnet development in progress

a) IR magnets for the HL-LHC

After an upgrade in the first long shutdown (LS1) during 2013-2015, the LHC has to deliver $\sim 300 \text{ fb}^{-1}$ of integrated luminosity at 13-14 TeV center-of-mass proton energy to both the CMS and ATLAS experiments. A plan for a luminosity upgrade (HL-LHC) aimed at collecting $\sim 3000 \text{ fb}^{-1}$ per experiment in the following 10 years was proposed [77]. To achieve this goal the low- β quadrupoles in the high luminosity IRs need to be replaced with quadrupoles of much higher performance based on Nb₃Sn technology [53].

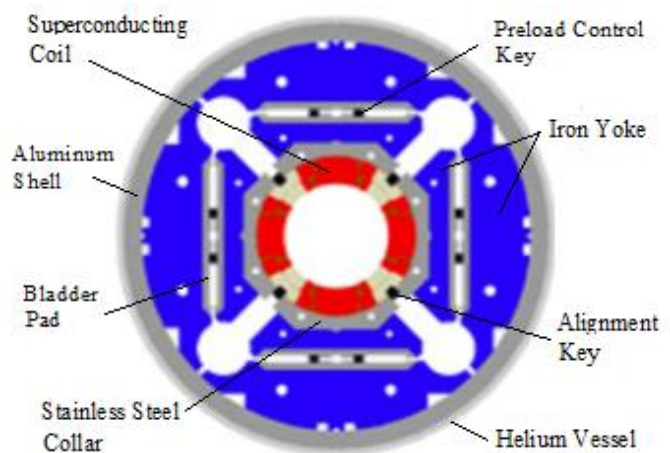


Fig. 15. The 150 mm QXF quadrupole.

The IR quadrupoles QXF feature a 150 mm aperture and a nominal field gradient of 140 T/m with a 20% operating margin at 1.9 K [78]. The quadrupole cross-section is shown in Fig. 15. The QXF nominal operating current is 17.46 kA. The maximum field in the coil is ~ 12.1 T and ~ 14.5 T at I_{nom} and the Short Sample Limit (SSL), respectively. The magnet uses a mechanical structure based on a thick Aluminum shell and key and water-pressurized bladder technique [79]. A Rutherford cable is made of 40 strands, 0.85 mm in diameter and incorporates a 12 mm wide and 0.025 mm thick stainless steel

core. The cable insulation is 0.15 mm thick and is made of S2-glass fibers braided directly on the cable.

The 1.5-m long QXF models are being developed by US-LARP and by CERN to be followed by a full-scale prototype and production. The first short models are being fabricated and will be tested in the second part of 2015. The first ~4 m long quadrupole prototypes will be produced and tested at the end of 2016 - early 2017. Magnet production will start in 2018 both in the U.S. and in the EU and is planned for 4 years [80].

The large QXF aperture influences the aperture and parameters of the separation and recombination dipoles [53]. Present 60 mm aperture normal D1 dipoles have to be replaced with 150 mm aperture superconducting dipoles operating at 78% of the conductor limit [81]. The D1 with appropriate shielding will decrease the distance between the D1 and D2 magnets to accommodate longer triplets and crab cavities. A 15 mm thick single layer NbTi coil is adopted for the D1 to provide a sufficient field while keeping the yoke width as wide as possible. The cross section of the new D1 magnet is shown in Fig. 16 [81]. Nb-Ti coils will provide an operational field of 5.6 T. The recombination dipoles D2 are twin-aperture magnets with the same integrated field of 35 T-m. The plan is to use Nb-Ti coils in these magnets with increased aperture, which is a challenge in a twin-aperture configuration.

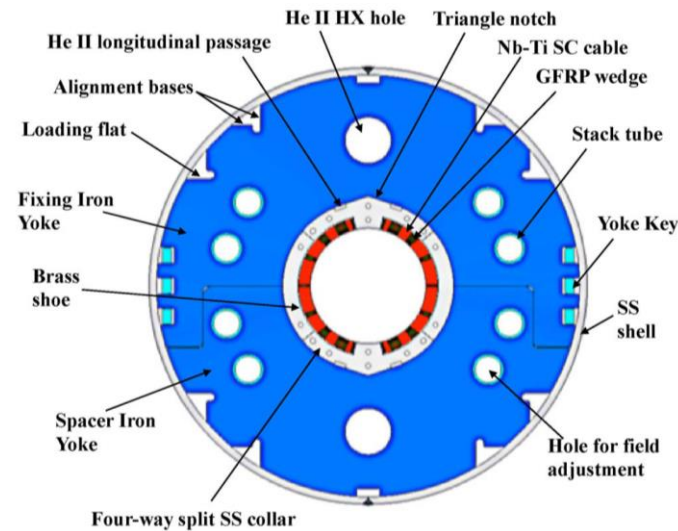


Fig. 16. Cross section of the superconducting separation dipole magnet D1 with a coil aperture of 150 mm.

b) 11 T dipoles for the LHC collimation system upgrade

Additional collimators are planned in the LHC dispersion suppressor areas around points 2, 3, 7, and CMS and ATLAS detectors [75]. Creating a space for these collimators requires replacing some 8.33 T, 15 m long Nb-Ti main dipoles (MB) with shorter 11 T Nb₃Sn dipoles (MBH) compatible with the LHC lattice and main systems, and delivering the same integrated strength at the LHC nominal operating current of 11.85 kA. CERN and FNAL are jointly developing a 5.5 m long twin-aperture 11 T Nb₃Sn dipole. Two of these magnets with a collimator in between will replace one MB dipole.

Design concepts of the 11 T Nb₃Sn dipole in both single-aperture and twin-aperture (Fig. 17) configurations are

described in [82], [83]. The dipole design features 2-layer shell-type Nb₃Sn coils, separate stainless steel collars for each aperture and a main dipole yoke modified at the collar-yoke interface. The magnet coil, made of a Rutherford cable with 40 strands, 0.7 mm in diameter and a 0.025 mm thick stainless steel core, was designed to provide a dipole field of 11 T with ~20% margin in a 60 mm aperture at the LHC nominal operating current and a temperature of 1.9 K, and low-order geometrical field harmonics inside a circle 34 mm in diameter. The 60-mm coil aperture is slightly larger than the main dipole aperture to avoid bending the Nb₃Sn coils. Using separate collars for each aperture simplifies magnet assembly and reduces the risk of coil damage during assembly.

Two meter long, single-aperture Nb₃Sn dipole demonstrators and a series of short models were fabricated and tested at FNAL during 2012-2014 [84]. The two 1-m long collared coils were assembled and tested at FNAL in a twin-aperture configuration and achieved a bore field of 11.5 T at 1.9 K which is ~97% of the magnet design field [85]. CERN started testing the first 2-m long single-aperture dipole models in 2014 [86]. Two twin-aperture models will also be tested during 2015-2016 before fabrication and test of a 5.5 m long twin-aperture 11 T dipole prototype. Magnet production is planned at CERN in collaboration with industry.

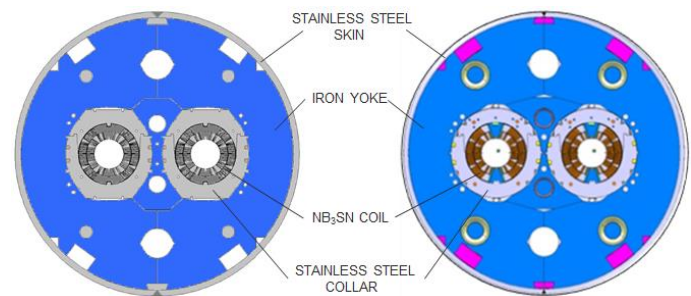


Fig. 17. Cross-sections of the 11 T DS dipole: FNAL design (left), CERN design (right).

c) IR magnets for future hadron colliders

The Very Large Hadron Collider (VLHC) has provisions for two large colliding experiments and two stages – VLHC-1 and VLHC-2 [33]. The IR quadrupoles form the final focus at the two collision points. The required gradient is ~300 T/m with a length of 10 m and a single aperture of ~80 mm. The field quality has to be very good due to a beam separation of up to 12.5 mm. VLHC-1 aims for a factor of 3 higher than the LHC energy at comparable luminosities. This could be accomplished by making a quadrupole similar to the LHC IR upgrades, with a small aperture but higher gradient. A two-layer design based on Nb₃Sn coils operating at 4.3 K is a realistic approach to meet the requirements for these magnets. Nb₃Sn quadrupole models with parameters close to this were developed by the US-LARP program in 2006-2009 [87].

In VLHC-2, two possible collision optics were discussed: one has symmetric doublet optics with flat beams and another one has traditional anti-symmetric optics with round beams [33]. In both cases the magnet parameters are quite challenging. All

these magnets require using Nb₃Sn technology and development of innovative magnet designs.

The IR design for the Future Circular Collider (FCC) is still at a very early stage [88].

III. LEPTON COLLIDERS

A. Electron-Positron Circular Colliders

Electron-positron circular colliders have been used extensively for high-energy particle physics. More than 20 e^+e^- colliders have been built [89]. The design of these machines is constrained by the level of synchrotron radiation, prohibiting the use of superconducting magnets in the arcs. However, superconducting magnets in final focus system, used in some machines, have enabled the achievement of high luminosity. Parameters and operation times of electron-positron colliders with superconducting IR magnets are summarized in Table IV. The IR quadrupoles (IRQs) in these machines have to be integrated into the experiments, imposing severe limitations on the magnet design. In particular, these magnets have to occupy minimum space in the transverse direction, have sufficient operating margin, and be supported together with other beam- and experiment-related equipment.

TABLE IV.
ELECTRON-POSITRON CIRCULAR COLLIDERS.

Collider	Location	Scheme*	Energy (GeV)	L (10^{32} cm ⁻² s ⁻¹)	Operation
TRISTAN	KEK	S	32	0.4	1986-1995
LEP	CERN	S	65	0.24	1989-1994
LEP2	CERN	S	105	1	1995-2000
CESRII	Cornell	S	1.9	0.6	2002-2008
BEPCII	IHEP	D	2.1	7.1	2007-
KEKB	KEK	D	3.5/8	211	1999-2010
SuperKEKB	KEK	D	4/7	8000	2016-

* S-single ring, D – double ring.

1) LEP/LEP2 IRQ

The low-beta insertions in LEP, the e^+e^- collider at CERN, consist of eight 2 m long superconducting quadrupoles embedded into each side of the four experiments. These iron-free magnets were designed to give the highest gradient obtainable with industrially-proven technology at the time [90], [91]. With the other elements of the insertions they covered the first phase of LEP operation up to 65 GeV. The LEP IR quadrupole is a warm-bore, bath-cooled magnet providing a maximum gradient of 36 T/m over a useful aperture of 100 mm diameter. It was designed to take full advantage of the experience gained from the successful development, fabrication and operation of the CERN ISR superconducting low-beta quadrupoles [17], [92]. Monolithic 1.8 mm by 3.6 mm composite conductor consisted of 1500 Nb-Ti 45 μ m filaments in a copper matrix (Cu/Sc=1.7). Each coil consisted of two blocks of insulated conductor separated by metal spacers. The 184 turns, were continuously wound in radial layers of 8 turns and grouped in 2 blocks of seven and sixteen layers and epoxy-impregnated. The coil azimuthal pre-load was achieved by means of Al shrinking rings. The cross-section of the magnet in the horizontal cryostat is shown in Fig. 18.

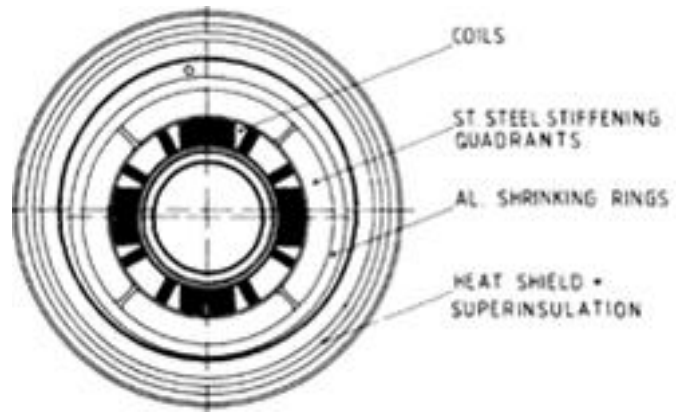


Fig. 18. Cross-section of the SC quadrupole in cryostat.

The magnet was cooled by pool-boiling helium at 4.25 K with the boil-off gas used to cool the current leads and screen. The magnet was suspended by tension rods connected to the vacuum vessel.

After the upgrade, the LEP2 project brought the machine energy up to 105 GeV with a factor of 4 higher luminosity. This was achieved by using stronger final focus quadrupoles [93]. LEP and LEP2 FF quadrupole parameters are compared in Table V. Thanks to the higher performance Nb-Ti conductor, it was possible to retain the external dimensions of the initial units. Nevertheless, to achieve the required 50% increase in integrated gradient, a number of significant changes have been made.

To keep the coil blocks under compression at 75% higher Lorentz forces, significant changes were made to the coil support structure. The space obtained by reduction of the coil dimensions was used to increase the stiffness of the coil support structure by using thick Al rings instead of a combination of longitudinal quadrants and thin shrink rings. Besides increasing the inertia, the thicker Al ring provides larger azimuthal prestress in the coil at low temperatures. Longitudinal stiffness of the magnet was achieved by using a three-point support attached to the 5 mm thick stainless steel helium vessel.

TABLE V.
LEP AND LEP2 IR QUADRUPOLE PARAMETERS.

Parameter	LEP	LEP2
G _{nom} (T/m)	21.7	76.37
Coil ID (mm)	130	50

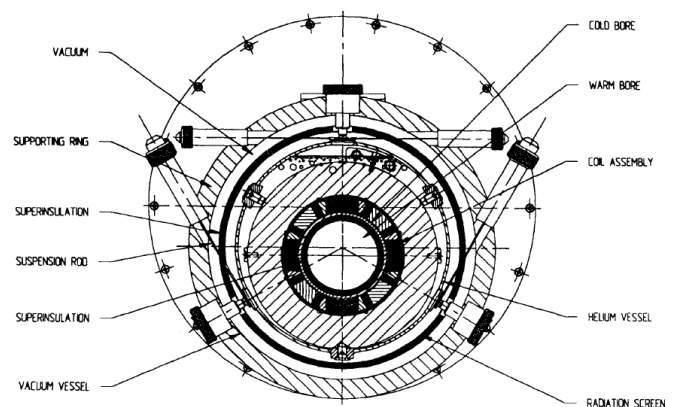


Fig. 19. LEP2 quadrupole cryostat cross-section.

The cross-section of the LEP2 quadrupole in the cryostat is shown in Fig. 19. The new cryostat has a modified main helium vessel and warm bore tube. It was changed from a thin corrugated structure to a 5 mm thick cylinder that serves both as an inertia support cylinder and a helium jacket.

2) CESR IRQ

The goal of the phase III upgrade of the CESR/CLEO was to increase the CESR luminosity from the $8 \cdot 10^{32} \text{cm}^{-1} \text{s}^{-2}$ to $1.7 \cdot 10^{33} \text{cm}^{-1} \text{s}^{-2}$. In order to minimize the long-range beam-beam tune shifts due to the small ± 2 mrad crossing angle the beam separation to horizontal width ratio must be maximized, and the β -functions at the crossing points must be minimized. The latter feature was achieved by placing the IR system as close to the IP as possible using high-gradient superconducting quadrupoles

[94]. One cryostat with two multifunctional superconducting magnets was installed on each side of the IP [95]. The IR layout is shown in Fig. 20. The cryostat has a warm bore with an ID of 145 mm and a maximum OD of 495 mm.

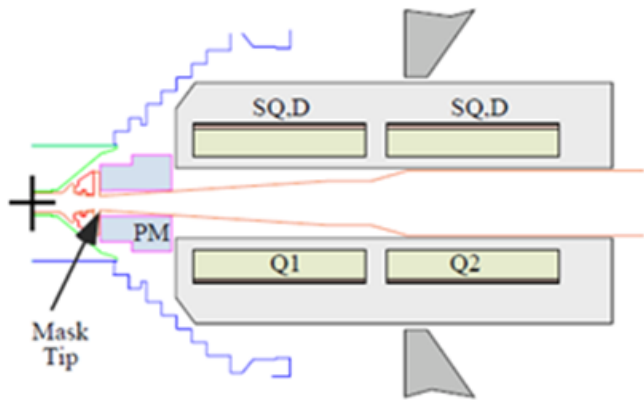


Fig. 20. IR layout showing 7 magnetic elements.

All four superconducting magnets are identical and consist of three independent sets of coils with effective lengths of 0.65 m. The Q1-Q2 gradient is 48.4 T/m at 1225 A. The skew quadrupole (SQ) field is ~ 5 T/m. The dipole coils produce a horizontal dipole field with a maximum strength of 0.13 T. The design of the Q1 and Q2 coils was highly influenced by the LEP200 IR quadrupoles [96], [93], especially in the choice of bore size and conductor. The other superconducting coils were loosely modeled after the LHC corrector magnets. The design current of all magnets was chosen to be less than 70% of the quench current limit under worst case conditions (multiple coils energized and the presence of the 1.5 T CLEO solenoid field). The magnets interact strongly with the detector solenoid magnetic field. Q1 is completely immersed in the 1.5 T solenoid field. The solenoid field and the current in the dipole generate a very large moment of 12,000 N-m on Q1. Q2 has one end in the solenoid fringe field while the other end is essentially field free, resulting in a net horizontal force on Q2 of up to 14,000 N. These forces were intercepted by the cryostat and a robust magnet support structure.

3) BEPS IR

BEPCII is an upgrade of the Beijing Electron and Positron Collider (BEPC). A new ring was installed next to the original in the existing tunnel to contain the electron and positron beams

separately. The BEPCII storage ring circumference is 238 m and the IR length is ~ 14 m around the interaction point. There is one superconducting magnet, one septum bending magnet, two twin aperture quadrupoles and four slim quadrupoles on each side of the IR [97].

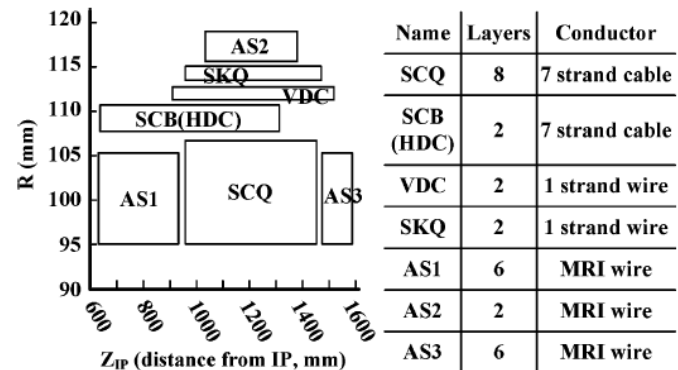


Fig. 21. BEPCII superconducting magnet coil layout and parameters.

TABLE VI.
BEPCII IR COIL DESIGN PARAMETERS

Coil	B (T) or G (T/m)	R _{in} -R _{out} (mm)	L _{coil} (mm)	I _{nom} (A)
SCQ	18.744	95.1-108.1	496	477
SCB	0.543	108.5-111.8	674	496
HDC	0.056	108.5-111.8	674	51
VDC	0.059	111.9-113.5	610	27
SKQ	0.937	113.6-115.2	510	47
AS1	-	95.1-105.9	303	1078
AS2	-	115.4-119.0	346	1078±55
AS3	-	95.1-105.9	116	1078±55

The closest magnet to the interaction point is a superconducting magnet, which is shared by both electron and positron beams. It sits in a 1 T, 3.6 m long BESIII detector solenoid. The magnet was designed by BNL and the Institute of High Energy Physics (IHEP) and built by BNL using a serpentine coil configuration, developed at BNL [98]. It has a multi-function coil package, shown in Fig. 21, which includes the main quadrupole SCQ, horizontal dipole SCB, vertical dipole VDC, skew quadrupole SKQ and three anti-solenoid windings AS1, AS2, and AS3. Table VI summarizes the design parameters of the superconducting coils. The cryostat has a 132 mm diameter warm bore and an outer diameter of 326 mm.

Magnetic measurements were performed at BNL in a vertical dewar and horizontal measurements were done at IHEP. During the vertical test and the subsequent commissioning test, all the coils reached 110% of their design currents. Operation of the superconducting magnets started in June 2007. There were no spontaneous quenches.

4) TRISTAN, KEKB, and Super KEKB IR quadrupoles

The low- β insertion quadrupoles in the TRISTAN and KEKB interaction regions are iron-free superconducting magnets. The TRISTAN quadrupoles have a gradient of 70 T/m with a 140 mm inner coil diameter and the KEKB quadrupoles have a gradient of 21.7 T/m with a 130 mm inner coil diameter [18],

[99]. The coil design is based on 4-layer $\cos 2\theta$ windings and 2-layer $\cos 2\theta$ windings, respectively, clamped and supported by stainless-steel collars. The experience with an air-core IR quadrupole magnet design at TRISTAN served as a useful basis for the KEKB IR magnet design, which was more strongly coupled with the particle detector system, and had to satisfy the requirements of the low-beta insertion design for increased luminosity. The KEKB IR quadrupole magnet cross section is shown in Fig. 22. From the inside, the main components are: a warm bore, inner thermal shield, inner wall of the helium vessel, correction coils, main quadrupole coil, 316LN stainless-steel collar, outer wall of the helium vessel, outer thermal shield and vacuum vessel. NbTi/Cu Rutherford cable for the coil winding is made with 24 multifilamentary strands of 0.59 mm diameter (Cu/SC ratio 1.8) with 6 μm filaments twisted with a pitch of ~ 60 mm.

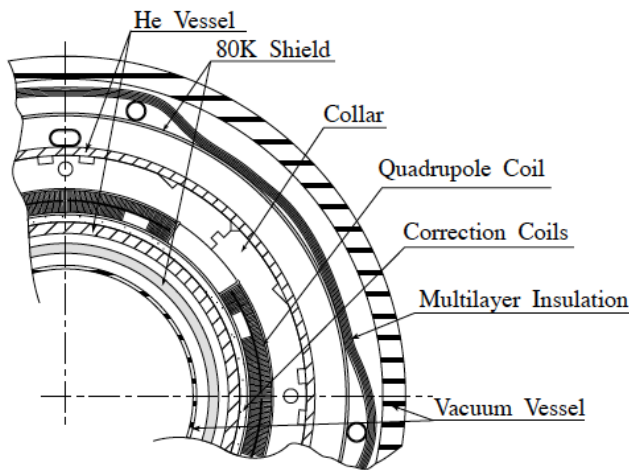


Fig. 22. A quarter cross section of a KEKB insertion quadrupole magnet.

The SuperKEKB [100] is an upgrade of the KEKB machine targeting a luminosity of $8 \cdot 10^{35} \text{ cm}^{-2} \text{ s}^{-1}$, 40 times higher than that achieved in KEKB. The accelerator design was based on the “nano-beam scheme” [101]. The beam optics was designed with a large horizontal beam crossing angle of 83 mrad and small beam sizes of ~ 50 nm at the interaction point, where the beam energies of e^- and e^+ are 7 GeV and 4 GeV, respectively. With these challenging parameters, the SuperKEKB IR system is the most important accelerator component. The system consists of 8 superconducting quadrupoles, 4 superconducting compensation solenoids [102], and 43 superconducting correctors fabricated by using a direct coil winding technique developed by BNL as explained later [103]. The beam is squeezed in the vertical and horizontal directions with the QC1 and QC2 quadrupoles, respectively.

The superconducting magnets are assembled into two cryostats that are located on both sides of the IP. The cryostats are installed inside of the particle detector, Belle II [104], and the IR final focus system is operated in the 1.5 T field of the detector solenoid. To reduce the effect of the solenoid field on the beam, superconducting compensation solenoids are used. The QC1 magnets are assembled in the compensation solenoid bore and operated under the combined field with the solenoid

magnets. The QC1 magnets for the e^+ beam line, QC1P, are located closest to the IP, and the QC1s for the e^- beam line, QC1E, are located behind the QC1Ps.

QC1P and QC1E are positioned as close to the IP as possible, and the magnet outer diameter is determined by the separation of the two beams at the IP side. QC1P and QC1E also have warm beam pipes, helium inner vessels and multi-layered superconducting corrector coils inside the magnet bores.

The cross sections of QC1P and QC1E are shown in Fig. 23, and the magnet parameters are listed in Table VII.

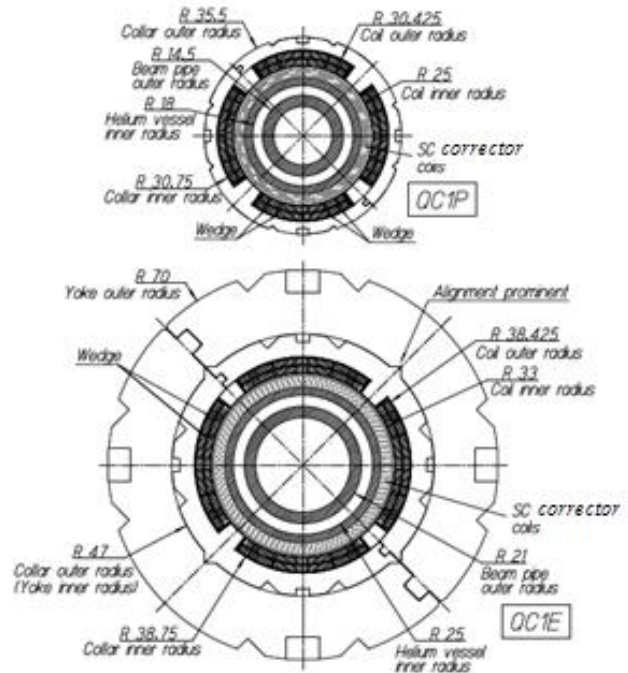


Fig. 23. Magnet cross sections of the QC1P and QC1E straight sections.

QC1P is designed as a collared ironless magnet. Each main quadrupole coil consists of two layers and three blocks. The four coils are clamped with non-magnetic collars. In the magnet bore, three superconducting corrector coils are wound on the inner helium vessel tube. Since QC1P does not have a magnetic yoke, its non-linear external field components, $b_3 - b_6$, are locally canceled at the neighboring beam via dedicated correctors with a field strength profile that varies rapidly with distance from the IP [103]. The design field gradient is 76.37 T/m at 1800 A. The QC1Ps are operated under combined solenoid fields of 2.60 T in the axial direction and 1.05 T in the radial direction, resulting in a peak field in the quadrupole coils of 4.56 T at 1800 A. The operating current at 4.7 K is 72.3% of the magnet critical current (short sample limit).

QC1E has magnetic yoke to enhance the quadrupole field strength and to reduce the field leakage from QC1Es to the e^+ beam line. The magnetic field strength in the yoke by the combined solenoid field was expected to be less than 1 T. The design field gradient of QC1E is 91.57 T/m at 2000 A.

The construction of superconducting quadrupoles QC1P and QC1E for the SuperKEKB beam final focusing system is complete [105].

TABLE VII.

PARAMETERS OF KEKB AND SUPERKEKB IR QUADRUPOLES.

Parameter	TRISTA	KEKB	Super KEKB	
	N		QC1P	QC1E
G_{nom} (T/m)	70	21.7	76.37	91.57
Coil ID (mm)	140	130	50	66

B. Linear Colliders

1) Quadrupoles in the ILC main linac.

The International Linear Collider (ILC) is proposed to be built as a next-generation e^+e^- collider based on superconducting RF (SRF) accelerator technology [106]. Superconducting magnet technology, however, is also required for beam focusing and steering along the main linac beam line. Superconducting quadrupole magnets are periodically installed between SRF accelerating structure strings. The basic design magnet features superferric quadrupole magnets with a split iron yoke for efficient assembly around the beam pipe in the cryomodule, and with race-track coils conductively cooled and attached to the cold iron pole [107]. Fig. 24 shows a cross section of the quadrupole magnet installed in a SRF cryomodule. The superferric quadrupoles have a peak gradient of 54 T/m with a 78 mm aperture [108], [109], [110].

A key requirement for the quadrupole magnet is stability of the magnetic center to be $<5 \mu$ for a 20 % dynamic change in the field gradient that is driven by beam dynamics feed-back requirements (beam-based alignment). This stringent requirement is met by incorporating a conduction-cooled and split-able magnet structure, eliminating the need for a liquid helium vessel, and an iron dominated field configuration.

As an additional advantage, the magnet assembly and installation may be installed around the beam pipe without disconnecting the SRF cavity strings. Thus it may eliminate possible contamination of the cavity RF surfaces inside the SRF cavity, and greatly simplify the SRF cavity string-assembly operation, eliminating the need for a clean room environment during the quadrupole magnet assembly.

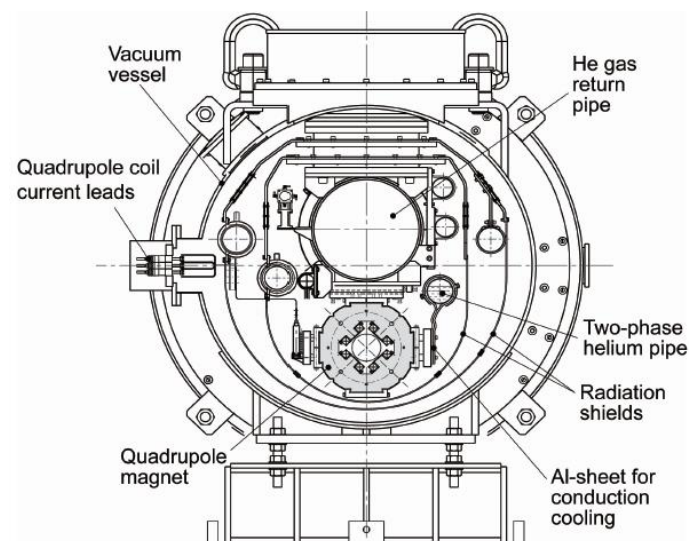


Fig. 24. Cross section of the ILC main linac quadrupole Cryomodule.

2) Quadrupoles for ILC IR

The ILC final focus (FF) at the IR requires a compact superconducting quadrupole magnet system for the incoming and outgoing beam lines, as close as possible to the beam interaction point (IP), as shown in Fig. 25, in order to minimize the beam size and to maximize the beam interactions at the IP [106], [111]. The ILC interaction region is complicated, since even with a 14 mrad crossing angle configuration the incoming/outgoing beams are in very close proximity.

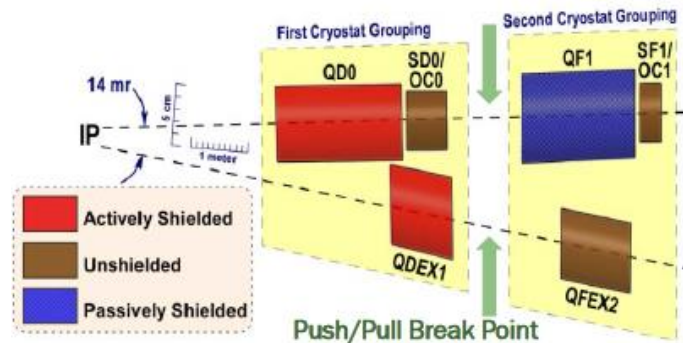


Fig. 25. Conceptual layout of the ILC IR final focus magnet system.

The ILC FF requirements differ significantly from those at other colliders. For a 250 GeV beam energy the maximum beam size in QD0, the closest quadrupole to the IP, is 0.220 mm horizontal and 0.063 mm vertical with a 10 mm radius beam pipe. QD0 has $45\sigma/158\sigma$ horizontal/vertical clear aperture [37], [111], [112]. Furthermore, since a given beam pulse passes only once through QD0, and then only samples a small central field region, the QD0 harmonic field quality requirements are extremely relaxed. The ILC final focus operating gradients are intentionally limited to 140 T/m to minimize synchrotron radiation generated by beam going to the IP. With the QD0's small inner coil radius, given in Table VIII, the coil peak field is modest, being less than 2 T. In addition to QD0's own field, the solenoidal background field from the detector additionally adds a few Tesla in quadrature. The relatively very large, in terms of beam sigma, 10 mm QD0 beam pipe radius is used for cleanly passing synchrotron radiation generated by beam halo at locations far upstream that could otherwise generate experimental background. Significantly reducing the QD0 clear aperture would require tighter upstream collimation that would then increase wake field induced emittance dilution and negatively impact ILC luminosity.

TABLE VIII
ILC QD0 DESIGN PARAMETERS.

	Main	Shield	Combined
Field gradient (T/m)	148	-8	140
Coil ID (mm)	24.2	67.0	24.2

All challenging aspects of the QD0 design requirements stem from Machine Detector Interface (MDI) issues. As specified in the ILC TDR, the QD0 distance to the IP, L^* (3.51 m for the SiD experiment and 4.50 m for ILD, recently converged to a common value of $L^* = 4.1$ m for both experiments) is such that QD0 must be supported by the detectors themselves. The ILC

14 mrad total crossing angle derives from a compromise between clean accelerator magnet separation of the incoming/outgoing beams while not losing transverse space (physics acceptance) inside the detector.

A photo made during winding a layer of the ILC QD0 R&D prototype via the BNL Direct Wind technique [113] is shown in Fig. 26. By using this computer-controlled machine all the turns for a given coil layer are put in place on a support structure before winding proceeds to the next layer. The full QD0 coil cross section has six inner layers that are run in series with a single reversed polarity larger radius outer layer and is shown in the inset of Fig. 26. The reversed current direction in the outermost active shield layer serves to cancel the QD0 external field outside the combined coil structure with only a 5.4% gradient reduction seen by the beam.

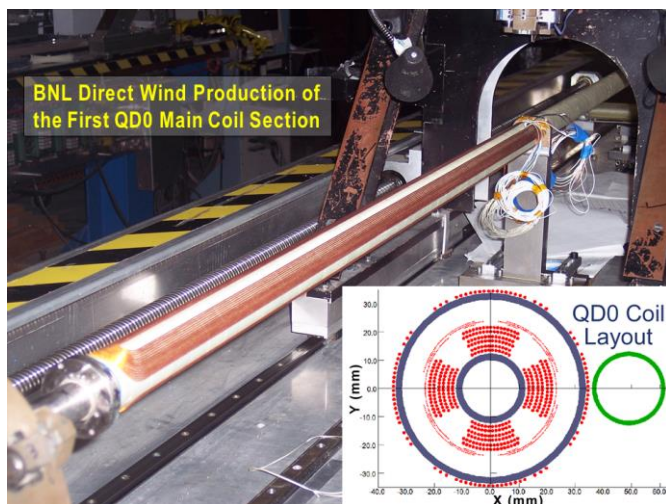


Fig. 26. A photo during winding a layer of the ILC QD0 prototype via the BNL Direct Wind technique, and a cross section of the main coil with compensation coils on the outer most layer.

In order to constrain deflection of the long aspect ratio support structure during production, QD0 is wound in two halves, rigidly supported at the center. In fact, special low beam energy optics will take advantage of this split to increase luminosity by reducing the gradient in the QD0 half farther from the IP while maintaining full gradient in the other half. This strategy reduces the effective L^* of the combined QD0 coils. Note that along with QD0, the QD0 cryostat also contains a sextupole/octupole coil package and the first extraction line quadrupole.

Overlapping the IP end of QD0 there is also a set of anti-solenoid coils. The anti-solenoid coils are not intended to wholly cancel the detector solenoid field but rather are configured to reduce high-order optics effects due to superposing the detector field and QD0 focusing. The anti-solenoid has a distinctive dual coil inner/outer opposite polarity coil geometry that dramatically reduces the net longitudinal repulsive force from the detector solenoid on the QD0 cold mass and at the same time diminishes the impact of the anti-solenoid's own external field on the detector field profile. Since sufficiently precise positioning of a massive, multi-ton experimental detector after a push-pull detector swap where the magnets inside the cryostat move as a unit cannot be guaranteed, each magnet was provided

with appropriate normal and skew harmonic correction coils.

The single most daunting ILC magnet challenge and main motivation for producing the QD0 R&D prototype is vibration stability. Knowing that the IP vertical spot size is 6 nm, one could naively expect that the vertical position of QD0 has to be kept stable at this same level in order not to lose luminosity. Fortunately the QD0 vertical vibration stability budget is “relaxed” to 100 nm at frequencies above 5 Hz thanks to use of beam-based feedback during the passage of the long ILC bunch trains. To try to avoid one potential source of vibration the ILC QD0 is cooled via 1.9K pressurized He-II for effective static cooling that does not depend upon flowing cryogenes. In future vibration stability tests, QD0 cryostat movement can be monitored via the combination of external geophones and laser interferometry while being compared to data from the geophones placed directly inside the cold mass. R&D is also underway to look at implementing a direct, dynamic magnetic field measurement of the QD0 magnetic center via an independently stabilized multi-turn pickup coil supported inside the QD0 aperture.

The baseline ILC IR magnets are based on a Nb-Ti wire and the “Direct-Wind” technology, requiring multiple conductor layers interleaved with the insulation. It may not be an optimal concept in terms of the heat transfer as the multiple layers of insulation impede the radial heat transfer out of the coil. In order to improve the coil thermal characteristics, a different solution based on Rutherford type cables was also proposed [114].

C. Muon collider

A high-energy, high-luminosity Muon Collider (MC) is a new class of lepton colliders with great discovery potential. High-field superconducting dipoles and quadrupoles are essential for the MC Storage Ring (SR) and Interaction Regions (IR) [57], [115]. All the magnets require Nb₃Sn superconductor to achieve the design operating parameters with sufficient margins to provide reliable machine operation. The required margin brings the maximum design field in the coils to the limit of the Nb₃Sn technology.

1) Magnets for a Muon Collider Storage Ring (MC SR).

The nominal operation field of the SR main dipoles is ~ 10 T reducing the ring perimeter and, thus, maximizing the number of collisions during the short muon lifetime. The superconducting coils in the MC need to be protected from showers produced by the decay electrons. The high level and distribution of heat deposition in the MC SR requires magnets either with large aperture to accommodate thick high-Z absorbers shielding the coils or with an open midplane (OM) to create a path for the decay electrons to high-Z absorbers placed outside the coils. Both magnet design concepts were carefully analyzed [110], [116]. Besides the lower operation margin, difficulties of handling the large vertical forces in coils with midplane gaps, and complicated coil cooling and quench protection, the dynamic heat load in OM dipoles is still large since the decay electrons have a transverse momentum too large to pass through the open mid-plane with a strong vertical defocusing field in the gap. Furthermore, for muon beam

energies above 1.5 TeV, a dipole component is also needed in the quadrupoles to mitigate the neutrino radiation problem. Achieving the required level of both quadrupole and dipole components in OM combined-function magnets has serious challenges. Thus, the decision was taken in favor of large aperture magnets with an internal absorber. The cross-sections of 150-mm aperture arc magnets with shell-type coils selected for a 1.5×1.5 TeV MC SR are shown in Fig. 27, [117].

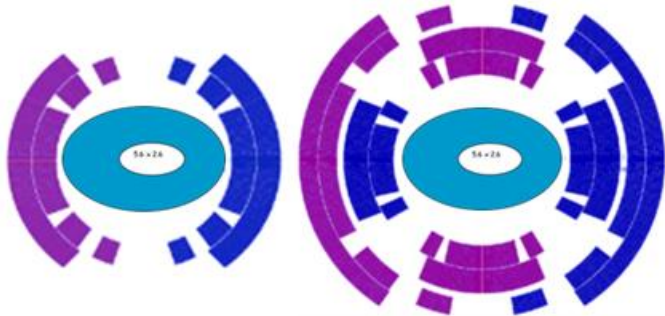


Fig. 27. 150-mm aperture dipole (left) and combined dipole/quadrupole coils (right) with thick elliptical internal absorber and shifted beam area.

2) MC IR magnets

The MC final focus (FF) system based on doublet and triplet layouts was studied in [118], [119]. The FF quadrupoles are based on two-layer shell-type coils with apertures from 80 to 180 mm [119]. Neutrino radiation is an important factor for a TeV-scale MC. In the quadrupoles nearest to the IP, the natural beam divergence is sufficient to spread it out, but in more distant quadrupoles an additional bending field of ~ 2 T is necessary. This bending field is created by special dipole coils. The IR quadrupole parameters are close to the LARP TQ, HQ and MQXF quadrupoles described above. However, for operation in a MC IR at 4.5 K with a reasonable operating margin these magnets require an increase in coil thickness. Larger-aperture quadrupoles (ID ~ 180 -200 mm) with dipole windings and IR dipoles will need focused R&D.

IV. BEAM LINES

A. J-PARC proton beam transport with combined-function magnets

The J-PARC proton synchrotron that delivers the neutrino beam to the T2K experiment needs a superconducting beam line to transport the 50 GeV primary proton beam to the secondary beam production target [120], [121]. It requires bending the primary proton beam by 80 degrees before producing and directing the neutrino beam toward Super-Kamiokande and the T2K experimental facility located 295 km west of J-PARC. The superconducting beam line consists of 28 superconducting combined function magnets, which are comprised of two (top and bottom) single layer left/right asymmetric coils that approximate a sum of a $\cos(\theta)$ and $\cos(2\theta)$ current configuration to provide a combined function dipole and quadruple field [36], [122], reducing the total number of magnet types required. The cross section of the magnet is shown in Fig. 28 and the magnet parameters are summarized in Table IX. The pole of the coil is tilted towards the high field side by about 20 degrees, resulting

in a left-/right asymmetric coil configuration. A pair of top and bottom coils produces a dipole field of 2.6 T, and a quadrupole field of 19 T/m [36, 123]. The coil is supported by plastic collars, which are made from fiberglass-filled phenol plastic. The plastic collars provide ground insulation as well as the reference for alignment with respect to the iron yoke structure.

TABLE IX.
PARAMETERS OF THE J-PARC COMBINED FUNCTION MAGNET

Parameter	Value
Dipole field (T)	2.59
Quadrupole field (T/m)	18.7
Coil peak field (T)	4.7
Coil ID (mm)	173

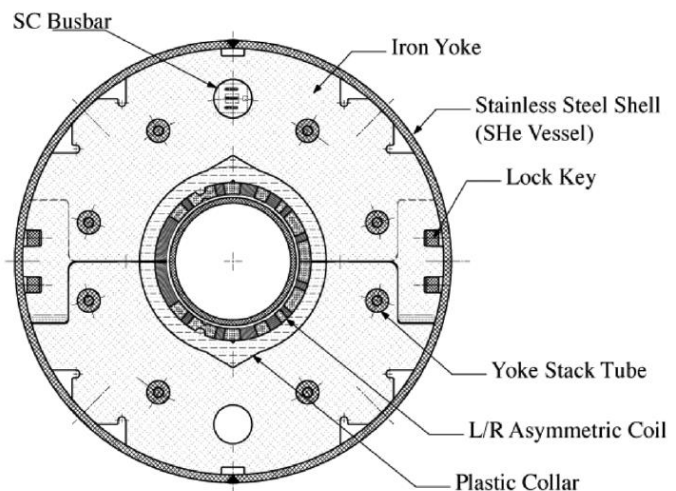


Fig. 28. Cross section of the combined function magnet for the J-PARC primary proton beam line.

To further simplify the system design and optimize cost, a two-in-one cryostat structure was adopted. Two identical magnets are longitudinally flipped in the cryomodule to form a quadrupole doublet, focusing and defocusing, function [124]. This configuration provides the same dipole field with no dipole field polarity change, but reversed polarity in the quadrupole field. All the magnets are excited in series with a single power supply.

The superconducting magnet system for the J-PARC neutrino beam line was successfully constructed and has been in steady operation for physics since 2010, with the exception of an unavoidable interruption resulting from the devastating earth quake that occurred in northern Japan, in 2011 [125].

B. Muon storage ring

1) BNL muon storage magnet

The muon g-2 experiment at BNL was carried out to determine the anomalous magnetic moment of the muon to a very high precision of < 0.5 parts per million (ppm), to examine a standard theory in particle physics [126]. The measurement requires a storage ring magnet with great stability and homogeneity. A superferric storage ring with a radius of 7.11 m and a magnetic field of 1.45 T was constructed in which the field quality was largely determined by the iron return yoke/pole and

superconducting coils with a continuous single ring structure [127]. Table X summarizes the main parameters, and Fig. 29 shows a cross section of the storage ring magnet.

TABLE X.
THE BNL MUON STORAGE RING MAGNET PARAMETERS

Parameter	Value
Nominal field (T)	1.451
Eq. orbit radius (m)	7.112
Nominal pole gap (mm)	180
Pole width (mm)	560
Muon storage region diameter (mm)	90

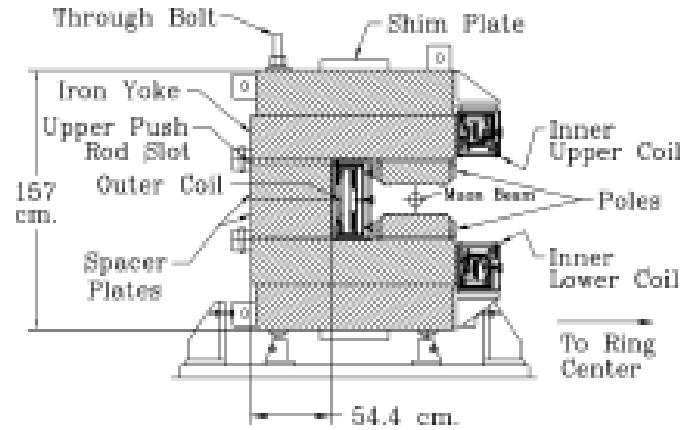


Fig. 29. A cross section of the BNL superferric single-ring magnet.

The magnetic field was excited with three superconducting ring coils using aluminum stabilized Nb-Ti superconductor originally developed for the TOPAZ experiment at the TRISTAN accelerator at KEK [128]. The coil at the outer radius drives the field across the storage ring gap, and two coils at the inner radius, above and below the mid-plane, cancel the flux in the ring center and improve the field quality in the gap. The storage ring was constructed with maximum attention to azimuthal symmetry and tight mechanical tolerances to obtain a homogenous magnetic field known to 0.1 ppm.

A superconducting inflector was developed for injecting pions/muons into the storage ring, to cancel the main dipole field from the injection beam line. It was also necessary to eliminate the external leakage field and minimize disturbance to the very uniform main magnetic field in the muon storage ring aperture just a few cm from the inflector beam channel as shown in Fig. 30. This was achieved by using a double $\cos\theta$ coil design for the magnetic field [129], [130]. It created a toroidal field and trapped most of the return field at the opposite side of the muon storage ring. The remaining small leakage field at the muon storage ring side was nearly perfectly shielded by using a special superconducting sheet which traps the remaining return field [131].

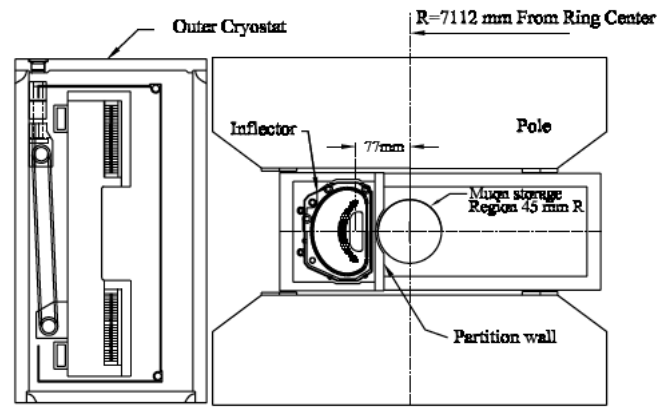


Fig. 30. Cross-section of the inflector magnet consisting of a double cosine theta coil providing a special toroidal field. The toroidal field in the injection beam bore is cancelled out via a dipole of opposite polarity to the main ring dipole.

The BNL muon magnet system was recently moved to Fermilab for the new muon g-2 experiment to be carried out to higher precision [132].

2) J-PARC muon storage ring

Another new experiment to measure g-2 aiming at a sensitivity down to 0.1 ppm is being prepared at J-PARC [133]. This experiment proposes a new approach, based on a much lower momentum of 300 MeV/c [134]. In the present design, a local uniformity of 1 ppm and an integral field uniformity of 0.1 ppm are required along the storage ring orbit, and the proposed field strength is 3 T [135], corresponding to a beam orbit of 33.3 cm in radius. Given the small radius of the beam orbit, the field strength and the field uniformity requirement, a compact, single superconducting solenoid can be tailored to serve as the muon storage ring.

A unique feature of the JPARC muon storage solenoid is to employ a spiral injection scheme, while the BNL experiment uses an inflector created by a radial fringe field around the end of the solenoid. The muon beam will be transported along the solenoid field from a hole in the iron yoke to the midplane in a spiral where the muons are extracted by an anti-Helmholtz type kicker magnet with a 1.3 Gauss, 150 ns wide pulse [135]. Finally, after several thousand turns in a 3 T magnetic field at the midplane, they will decay, resulting in a measurement of g-2 with unprecedented precision.

Table XI summarizes the experiment in progress at BNL and plans at Fermilab and KEK-JPARC along with the required superconducting magnet parameters.

TABLE XI.
PARAMETERS OF MUON G-2 STORAGE RINGS
AND SUPERCONDUCTING MAGNETS.

Parameter	BNL/FNAL	KEK-JPARC
Muon momentum (GeV/c)	3.09	0.3
SR nominal field (T)	1.45	3.0
SR radius (m)	7.11	0.33
Focusing field	Electric	Magnetic

V. SOME SPECIAL MAGNETS

A. RHIC helical dipole

Helical dipoles are used in RHIC to control the spin of the polarized protons. The design incorporates a 4 T dipole rotating through 360 degrees along a magnetic length of 2.4 m [136], [137]. Four of these magnets assembled in a group form 4 “Snakes” to control spin in the lattice and 8 “Rotators” to orient the spin axially at two collision points. A 3D view of the helical dipole cross-section is shown in Fig. 31. A low nominal current of 320 A was used to minimize the heat load through the current leads. The normalized design field harmonics are less than 10^{-3} with an allowed magnet rotation error of two degrees.

The coil structure consists of two thick aluminum cylinders with helical slots filled with Kapton-insulated cable made of 7, 0.33 mm diameter Nb-Ti strands. The innermost conductor has an ID of 100 mm. The tubes are surrounded by a single-piece iron yoke 356 mm in diameter. The yoke laminations have rectangular slots to house tie rods, warm-up heaters, helium flow, and magnet interconnect buses. Azimuthal and axial Lorentz forces are contained in the individual slots and the radial forces are contained by the yoke.

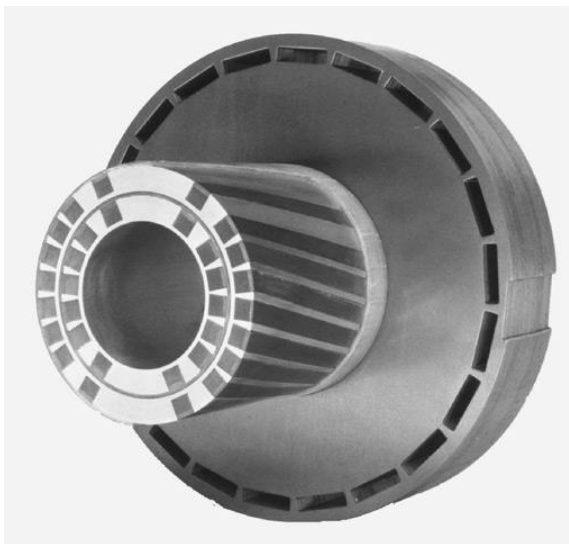


Fig. 31. A section cut from a prototype helical dipole.

B. Superconducting Magnets for Light Sources

Light sources were one of the early beneficiaries of the high fields provided by superconducting technology, albeit for very specific applications. The primary applications are superconducting wigglers, undulators and superconducting high field bend magnets used as insertion devices (IDs) to extend the spectral range of synchrotron light sources toward the hard (x-ray) end of the spectrum and increase brightness [138]. The wigglers and undulators consist of arrays of alternating magnetic fields that bend the electrons back and forth generating an emission in a narrow cone with an angular distribution of $1/\gamma$. The magnet array is placed as close to the beam as possible to generate the highest field without adversely perturbing the electron beam. Wigglers create beam deflections that are large compared to the natural emission angle of the synchrotron radiation and are generally several meters long. Wavelength

shifters are wigglers with a few poles that shift the radiation spectrum toward shorter wavelengths instead of increasing the intensity with a large number of bends. Single bend magnets are also used to harden the photon spectrum and are sometimes referred to as “superbends.” Magnets of this type were installed in the Advanced Light Source at Lawrence Berkeley National Laboratory in 2001 [139]. An undulator produces deflections comparable to the natural emission angle of the synchrotron radiation resulting in coherent interference and a narrow beam of photons peaked in narrow energy bands in harmonics of the fundamental frequency.

Superconducting wigglers and undulators, both have zero first and second order integrals along the particle orbit, and thereby have no effect on the operation of the storage ring. The main parameter that defines the radiation property of a wiggler or undulator is the K -value:

$$K = 0.934 \cdot \lambda_0 B_0,$$

where λ_0 is the field period in cm and B_0 is the field amplitude in Tesla. $K \sim 1$ corresponds to an undulator and $K \gg 1$ to a wiggler.

Superconducting insertion devices can provide fields 2 – 3 times higher using Nb-Ti compared to permanent magnets for the same pole gap and period. A comparison of field versus period for superconducting and permanent magnet design options is shown in Fig. 32. The first superconducting multi-pole wiggler was built by the Budker Institute for Nuclear Physics in 1979 and was installed in the 2 GeV storage ring VEPP-3 to increase the photon flux at shorter wavelengths [140]. The first undulator was built and installed in the ACO storage ring in the same timeframe [141].

Over the next few decades a number of wigglers and a few undulators were built and installed in second and third generation storage rings using superconducting technology. Despite the advantages of higher fields, obstacles such as lack of cryogenic infrastructure, very precise tolerance requirements over long lengths and tunability, have hindered widespread acceptance of the technology, particularly the more challenging undulators. However, there has been increasing interest in developing superconducting undulators for FELs because of a significant impact on performance and/or undulator length. Other motivations for using superconducting undulators are avoidance of radiation damage of permanent magnet material, allowing longer life and smaller gaps, possible reduction of resistive wakefield effects with a cold bore, smaller footprint and simpler K -control compared to the typical massive adjustable-gap permanent magnet undulators [142]. Additionally, the considerable improvement in cryo coolers greatly simplifies installation and operation.

Some R&D efforts are now taking further advantage of the high field properties of Nb₃Sn and HTS materials [143], [144]. A prototype undulator structure is shown in Fig. 33. Lawrence Berkeley National Laboratory [LBNL] is working on development of a superconducting undulator based on HTS tapes [145]. With a few more years of development, this technology will have a significant impact on light source design and performance.

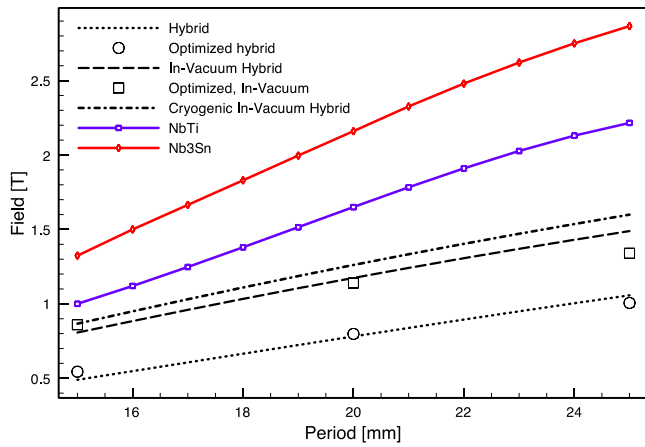


Fig. 32. Performance comparison of undulator technologies.

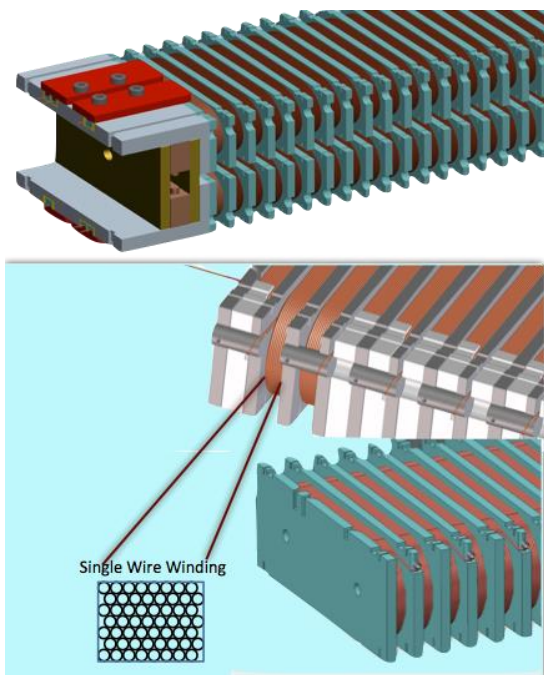


Fig. 33. Prototype of a Nb₃Sn undulator structure.

C. Superconducting Gantries for Cancer Therapy

A relatively recent application of superconducting accelerator magnets is toward development of compact, light-weight gantries for particle beam cancer therapy. Rotatable accelerator beamlines are preferred for modern particle therapy as they allow scanning and directing the beam at tumors from various angles, minimizing dose to healthy tissues surrounding the tumor. Current gantry designs rely on a resistive, ninety-degree bending magnet at the end of the gantry. The gantry used at the Heidelberg Ion Therapy Center weighs over 600 tons, motivating the use of superconducting magnet technology. Magnets for this application must have a large bore to accommodate a range of scanning angles, be significantly curved, combine bending and focusing and change field quickly for the energy variation required during treatment.

A superconducting gantry system is being developed in a collaboration led by the National Institute of Radiological Science (NIRS) in Japan. It will be installed as a therapy beam line at the Heavy Ion Medical Accelerator in Chiba (HIMAC) at NIRS, and the general layout is shown in Fig. 34 [146], [147], [148]. A cryo-cooled, combined-function, curved superconducting magnet system has been completed [149].

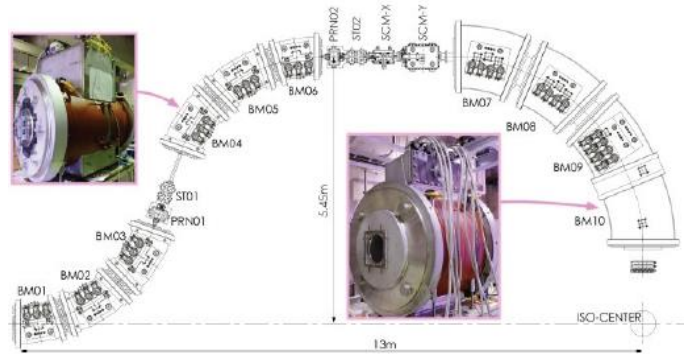


Fig. 34. Layout of the superconducting gantry system being developed at NIRS-HIMAC.

A team at the Lawrence Berkeley National Laboratory has been developing a design based on a concept first proposed by Meyer and Flasck, [150], [151], [152], [153], [154], [155], [156], [157]. The design, dubbed by the Berkeley group “canted cosine-theta” or CCT, is comprised of two nested solenoids with oppositely tilted windings. In the basic design, the layers are powered such that the solenoid components cancel leaving a nearly perfect dipole field, Fig. 35. For this application the conductor path is modified to create a pure dipole field with quadrupole and sextupole contributions.

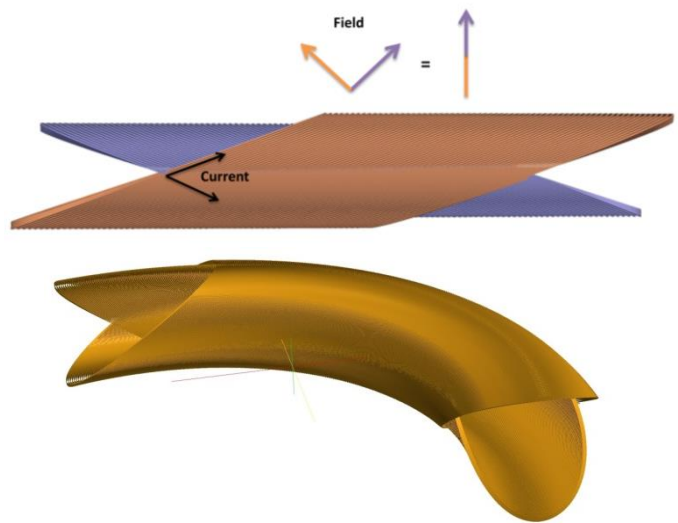


Fig. 35. Tilted solenoid dipole concept.

The LBNL design has a bore field of 3.5 T with a 130 mm bore and a 634 mm bending radius. A minimal symmetry allows constructing the winding mandrel in small sections or laminations. This feature has the advantages of simplifying assembly of the curved structure and reducing eddy currents

produced when the magnet is ramped. A prototype to demonstrate the basic concept is planned for the near future, [158]. [151].

D. Electron Cyclotron Resonance (ECR) Sources

ECRs are plasma-based ion sources used to inject intense, high charge state beams into heavy-ion drivers. Early sources were based on water-cooled copper solenoids and permanent magnet sextupoles. In the 1980's, Geller [159] predicted that beam currents would scale as the frequency squared and this has proven to be the case so far. The electron cyclotron resonance condition is

$$B_{ecr} = f_{RF}/28,$$

where B_{ecr} is in Tesla and f_{RF} is the RF frequency in GHz. Conventional technology is limited to around 18 GHz. Using Nb-Ti superconductors increases the limit to 28 GHz. There are currently four of these 3rd generation sources in the world: Michigan State University, RIKEN, Lanzhou and LBNL [160].

The VENUS source at LBNL was the first to achieve the required fields and has made feasible the current design of FRIB [161], [162], which requires up to 400 kW of beam power. This is at the limit of present 3rd generation sources. Both LBNL and Lanzhou are starting efforts to develop 4th generation sources based on Nb₃Sn which would reach frequencies up to 60 GHz [163], [164]. The coil structure for the LBNL ECR magnet is shown in Fig 36.

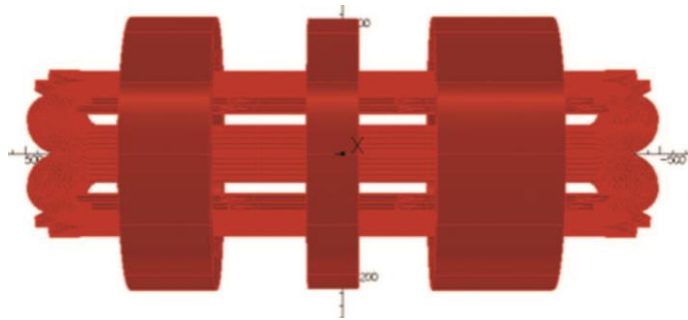


Fig. 36. Coil structure for the LBNL 4th generation ECR using six Nb₃Sn racetrack sextupole coils nested inside three solenoid coils that provide the axial field confinement.

E. Superferric magnets, spectrometers and other applications

Superconducting magnets are not confined to high field dipoles and high gradient quadrupoles dedicated to the energy frontier. Much alike the widespread use of superconductivity in detector magnets, which are outside of the scope of this paper, situation often arise where the required field volume of the magnet becomes very large, too large for a normal conducting electromagnet to be a practical solution.

Spectrometer dipole magnets are one typical such example. In spectrometers the beam acceptance has to be very large, by the necessity of bending beams with a ratio of energy over charge that can be very different. In addition, the poles gap is often relatively large to allow for beams of large emittance and reduce the direct energy deposition from beam losses into the magnet. The power consumption of a normal conducting electromagnet, for non-saturated iron, increases linearly with the iron gap and

the field generated. In addition, the overall mass of the magnet grows more than linearly with the width of the pole.

At a certain value of the field, and gap dimension, the size of the coil, of the iron, and the power consumption for a resistive electromagnet become so large that it is convenient to switch to a design based on a superconducting, cryostated coil. The exact trade-off depends on the specific of the beam energy, species, and optics, but it is typically in the range of 1.5 T field and 100 mm gap. In this range, the field can still be generated mainly by the iron yoke, whose shape and accuracy determine the field and field homogeneity, while the superconducting coil has the sole function of providing the required Ampere-turns in a more compact and efficient manner. This has the advantage of achieving very good field quality over a relatively wide range of field, as required by a good spectrometer. Besides dimensions and power consumption, the use of a superconducting coil adds to operational flexibility, allowing for operation at constant field with no overhead on the powering.

These so-called *superferric* magnets find most applications in large acceptance beam transfer and analysis lines, and spectrometers of radioactive and non-radioactive beams. An excellent example of one such facility is the analysis beam line and S800 spectrograph at the National Superconducting Cyclotron Laboratory (NSCL, USA) [165]. With an iron pole gap of 70 mm, a pole width of 450 mm and a nominal field in the aperture of 1.7 T, the dipoles of the beam line fall in the range identified earlier [166]. The beam line is used both as a transfer line towards the spectrometer, as well as a fragment separator for radioactive ions, which is the reason for the large aperture. The spectrometer S800 bends the beam in the vertical plane and was designed to reduce size and mass. It consists of two curved dipoles, of 75 tons each, where the coils follow the approximately 90 degree bent beam trajectory. The realization of the coil, and especially the negative curvature limb, demanded developing special techniques (clamping, hydraulic piston to maintain the coil geometry).

The most spectacular example of a superferric spectrometer is the SAMURAI magnet (Superconducting Analyzer for Multi-particles from Radioisotope beams), in operation at the RIKEN RI Beam Factory (Japan) since 2012, Fig. 37, [167].

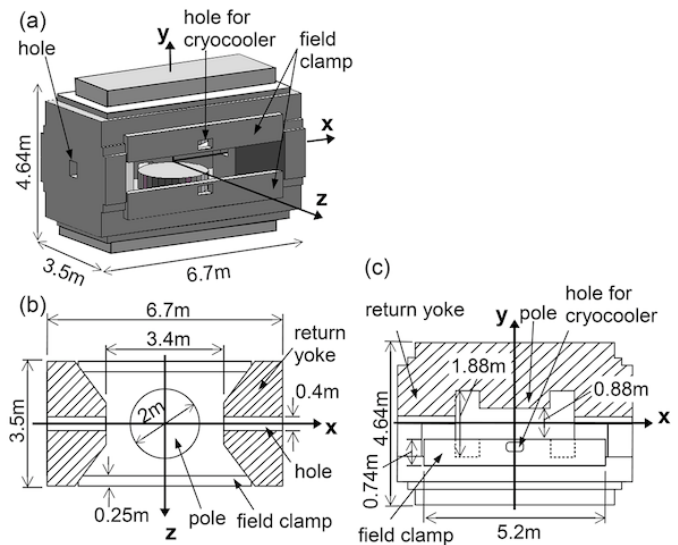


Fig. 37 Schematic view of the SAMURAI spectrometer, showing the large size yoke (a) and aperture (b), the round poles, and the cavity for the cryo-cooled Nb-Ti coils (c). By courtesy of RIKEN, Nishina Center, Japan, available at <http://www.nishina.riken.jp/RIBF/SAMURAI/config.html>

The 650 ton, 4.6 m tall dipole has a footprint of 6.7 m x 3.5 m, round poles of 2 m diameter, and a very large gap of 880 mm. The field in the gap is 3.1 T, for a peak field in the round Nb-Ti coils of 5.4 T. An additional feature of this large size spectrometer is that the magnet is mounted on a rotating platform that allows varying the angle of the aperture axis with respect to the position of the beam target and the detectors. To avoid the complication of movable cryogenic transfer lines, the magnet is initially cooled by liquid, until the shields and the two coils reach working condition and the coil cryostats are filled with 240 l of LHe each. Operation then switches to four GM/JT cryocoolers that maintain the temperature of the 77 K and 20 K shields, the current leads, and recondense the boil-off from the coil cryostats. Given the large stored energy (27 MJ) and inductance (up to 400 H), the magnet is subdivided and actively protected by heaters.

Among the present construction projects, the Super Fragment Separator (Super-FRS) at FAIR (Germany) is the one with the largest size [168]. The Super-FRS will require 24 large size superferric dipoles [169]. With a pole gap of 170 mm, a pole width of 450 mm, and an aperture field of 1.6 T, the Super-FRS dipole falls within the range identified earlier, where a superconducting coil is more efficient than a resistive electromagnet. The dipole has a weight of 50 tons, and the trapezoidal superconducting coils will be wound using Nb-Ti wire-in-channel conductor, cooled by a bath of LHe. A prototype of the Super-FRS dipole was tested successfully [170], and production is imminent.

Some of the features of superferric magnets are interesting beyond the use for large aperture beam transfer lines, separators and spectrometers that we described above. The fact that the iron dominates the field can be used to reduce the AC loss associated with fast cycled operation. We have described earlier the superferric magnet designs adopted at the Nuclotron, and FAIR. Similar work was pursued at CERN [171] and is the baseline for the NICA upgrade of the Nuclotron facility [172]. The use of HTS materials may offer additional advantages in terms of operating margin and energy efficiency [173].

Similarly, superferric magnets were considered as a low-cost option for collider projects such as the SSC [174], VLHC [175], and more recently the booster of the FCC-hh [176]. In this context, the main innovation was to combine the idea of an iron dominated magnet with a simplified, single-turn excitation provided by a high-current cable, similar to a transmission line. The concept is interesting in that it provides for a much simplified technology that could be applied to very long magnetic lengths, avoiding the need of magnet interconnects, and improving the magnet filling factor of the accelerator.

VI. CONCLUDING REMARKS

Superconducting accelerator magnet technology is celebrating its 50th anniversary and is still a rapidly developing field. After decades of successful development and implementation of superconducting accelerator magnets based

on low temperature superconductors such as Nb-Ti and Nb₃Sn, new exciting opportunities are being opened after the discovery of high-temperature (which are also high-field) superconductors and the development of practical HTS materials. These opportunities include both continued advancement toward higher magnetic fields and increased operating temperature.

This article was not intended to be a complete description of all aspects related to superconducting accelerator magnet designs and applications. Thousands of articles devoted to this technology, including reviews and technical reports, are presented annually at national and International Particle Accelerator Conferences (NA-PAC/IPAC), Magnet Technology Conference (MT), Cryogenic Engineering/Materials Conference (CEC/ICMC), Applied Superconductivity Conferences in the U.S. (ASC) and Europe (EUCAS), workshops and symposiums. All these sources are recommended to the readers who would like to further expand their knowledge in the area of superconducting accelerator magnets and their applications.

ACKNOWLEDGMENT

S.A. Gourlay thanks C. Lyneis, I. Pong, S. Prestemon, S. Sen, Lawrence Berkeley National Laboratory.

A. Yamamoto thanks V.S. Kashikhin of Fermilab, B. Parker of BNL, and K. Tsuchiya, N. Ohuchi, T. Ogitsu, T. Nakamoto, and K. Sasaki of KEK.

REFERENCES

- [1] M. H. Blewett, "Magnet Design in High-Energy Accelerators," *Nuclear Science, IEEE Transactions on*, vol. 12, pp. 317-326, 1965.
- [2] T. H. Fields and C. Laverick, "Some Supermagnet Design Considerations," *Nuclear Science, IEEE Transactions on*, vol. 12, pp. 362-366, 1965.
- [3] Z. Stekly and J. Zar, "Stable superconducting coils," *IEEE Transactions on Nuclear Science*, vol. 12, pp. 367-372, 1965.
- [4] "200 BeV Accelerator Design Study," UCRL-16000, June 1965.
- [5] A. Yamamoto and T. Taylor, "Superconducting Magnets for Particle Detectors and Fusion Devices," *Reviews of Accelerator Science and Technology*, vol. 5, pp. 91-118, 2012.
- [6] "1968 summer study on superconducting devices and accelerators at Brookhaven National Laboratory, BNL Internal Publication (unpublished) BNL 50155 (C-55), April 1969."
- [7] J. P. Blewett, "Panel Discussion on Superconducting Synchrotrons," *Nuclear Science, IEEE Transactions on*, vol. 18, pp. 628-628, 1971.
- [8] W. S. Gilbert, "Summary of International Progress on Superconducting Magnets," *Nuclear Science, IEEE Transactions on*, vol. 20, pp. 668-674, 1973.
- [9] W. B. Sampson, "Superconducting Synchrotron Magnet Development at Brookhaven," *Nuclear Science, IEEE Transactions on*, vol. 18, pp. 634-635, 1971.

- [10] R. L. Martin, "Comments on Superconducting Synchrotrons," *Nuclear Science, IEEE Transactions on*, vol. 18, pp. 632-633, 1971.
- [11] P. F. Smith, "Superconducting Synchrotron Development: Notes on Recent Work at the Rutherford Laboratory," *Nuclear Science, IEEE Transactions on*, vol. 18, pp. 641-641, 1971.
- [12] (2015). *Spear History*. Available: <http://www-ssrl.slac.stanford.edu/content/spear3/spear-history>
- [13] F. E. Mills, "Isabelle Design Study," *Nuclear Science, IEEE Transactions on*, vol. 20, pp. 1036-1038, 1973.
- [14] P. F. Dahl, R. Damm, D. D. Jacobus, C. Lasky, A. D. McInturff, G. H. Morgan, *et al.*, "Superconducting Magnet Models for Isabelle," *Nuclear Science, IEEE Transactions on*, vol. 20, pp. 688-692, 1973.
- [15] W. B. Fowler, D. Drickey, P. J. Reardon, B. P. Strauss, and D. F. Sutter, "The Fermilab Energy Doubler, A Two-Year Progress Report," *Nuclear Science, IEEE Transactions on*, vol. 22, pp. 1125-1128, 1975.
- [16] W. S. Gilbert, R. B. Meuser, W. L. Pope, and M. A. Green, "ESCAR Superconducting Magnet System," *Nuclear Science, IEEE Transactions on*, vol. 22, pp. 1129-1132, 1975.
- [17] J. Billan, K. N. Henrichsen, H. Laeger, P. Lebrun, R. Perin, S. Pichler, *et al.*, "A Superconducting High-Luminosity Insertion in the Intersecting Storage Rings (ISR)," *Nuclear Science, IEEE Transactions on*, vol. 26, pp. 3179-3181, 1979.
- [18] K. Tsuchiya, K. Egawa, K. Endo, Y. Morita, N. Ohuchi, and K. Asano, "Performance of the eight superconducting quadrupole magnets for the TRISTAN low-beta insertions," *Magnetics, IEEE Transactions on*, vol. 27, pp. 1940-1943, 1991.
- [19] A. Ageyev, V. Balbekov, Y. P. Dmitrevsky, A. Dunaitsev, Y. S. Fedotov, V. Gridasov, *et al.*, "The IHEP accelerating and storage complex (UNK) status report," in *11th International Conference on High-Energy Accelerators*, 1980, pp. 60-70.
- [20] J. S. Fraser and P. Tunnicliffe, "A study of a superconducting heavy ion cyclotron as a post accelerator for the CRNL MP Tandem," Atomic Energy of Canada Ltd., Chalk River, Ontario. Chalk River Nuclear Labs. 1975.
- [21] H. Blosser, "30 years of superconducting cyclotron technology," 2005.
- [22] S. Brandenburg, "The superconducting cyclotron AGOR: accelerator for light and heavy ions," in *Proc. PAC*, 1987.
- [23] H. Schreuder, "Recent developments in superconducting cyclotrons," in *Particle Accelerator Conference, 1995., Proceedings of the 1995*, 1995, pp. 317-321.
- [24] Y. Yano, "Status of the RIKEN RIB Factory," in *Particle Accelerator Conference, 2007. PAC. IEEE*, 2007, pp. 700-702.
- [25] H. Okuno, J.-i. Ohnishi, N. Fukunishi, T. Tominaka, K. Ikegami, A. Goto, *et al.*, "Magnets for the RIKEN superconducting ring cyclotron," in *Proc. 17th Int. Conf. on Cyclotrons and Their Applications, Tokyo*, 2004, pp. 373-377.
- [26] B. H. Wiik, "Hera, a New Stage in Colliding Beam Facilities," *Nuclear Science, IEEE Transactions on*, vol. 28, pp. 2020-2024, 1981.
- [27] P. A. Thompson, J. Cottingham, P. Dahl, R. Fernow, M. Garber, A. Ghosh, *et al.*, "Superconducting Magnet System for RHIC," *Nuclear Science, IEEE Transactions on*, vol. 32, pp. 3698-3700, 1985.
- [28] A. M. Baldin, S. A. Averichev, Y. D. Beznogikh, A. M. Doniagin, E. I. Djachkov, I. B. Issinsky, *et al.*, "Nuclotron Status Report," *Nuclear Science, IEEE Transactions on*, vol. 30, pp. 3247-3249, 1983.
- [29] M. Tigner, "Where Is the SSC Today?," *Nuclear Science, IEEE Transactions on*, vol. 32, pp. 1556-1560, 1985.
- [30] R. B. Palmer, "Design of superconducting magnets for the SSC," in *Particle Accelerator Conference, 1991. Accelerator Science and Technology., Conference Record of the 1991 IEEE*, 1991, pp. 32-36 vol.1.
- [31] L. R. Evans, "LHC status and plans," in *Particle Accelerator Conference, 1997. Proceedings of the 1997*, 1997, pp. 61-65 vol.1.
- [32] G. Dugan, "Very large hadron collider R&D," in *Particle Accelerator Conference, 1999. Proceedings of the 1999*, 1999, pp. 48-52.
- [33] G. Ambrosio, *et al.*, *Design Study for a Staged Very Large Hadron Collider*. Available: <http://www.slac.stanford.edu/pubs/slacreports/reports/06/slac-r-591.pdf>
- [34] P. Spiller, "Challenges and Progress in the Fair Accelerator Project," in *Particle Accelerator Conference, 2005. PAC 2005. Proceedings of the, 2005*, pp. 294-298.
- [35] K. Hasegawa, "J-PARC Commissioning Results," in *Particle Accelerator Conference, 2005. PAC 2005. Proceedings of the, 2005*, pp. 220-224.
- [36] T. Nakamoto, Y. Ajima, Y. Fujii, N. Higashi, A. Ichikawa, N. Kimura, *et al.*, "Development of Superconducting Combined Function Magnets for the Proton Transport Line for the J-PARC Neutrino Experiment," in *Particle Accelerator Conference, 2005. PAC 2005. Proceedings of the, 2005*, pp. 495-499.
- [37] B. Parker, M. Anerella, J. Escallier, M. Harrison, P. He, A. Jain, *et al.*, "Compact Superconducting Final Focus Magnet Options for the ILC," in *Particle Accelerator Conference, 2005. PAC 2005. Proceedings of the, 2005*, pp. 1569-1571.
- [38] R. R. Wilson, "The Tevatron, Fermilab Report TM-763," 1978.
- [39] R. Meinke, "Superconducting magnet system for HERA," *Magnetics, IEEE Transactions on*, vol. 27, pp. 1728-1734, 1991.
- [40] M. Anerella, J. Cottingham, J. Cozzolino, P. Dahl, Y. Elisman, J. Escallier, *et al.*, "The RHIC magnet system," *Nuclear Instruments and Methods in Physics Research Section A: Accelerators, Spectrometers, Detectors and Associated Equipment*, vol. 499, pp. 280-315, 2003.
- [41] L. Evans and P. Bryant, "LHC Machine," *Journal of Instrumentation*, vol. 3, p. S08001, 2008.

- [42] F. Zimmermann, "Challenges for Highest Energy Colliders," in *International Particle Accelerator Conference*, Dresden, Germany, 2014, pp. 1 - 6.
- [43] A. W. Chao and W. Chou, *Reviews of Accelerator Science and Technology* vol. 5, 2012.
- [44] A. Tollestrup and E. Todesco, "The development of superconducting magnets for use in particle accelerators: From the Tevatron to the LHC," *Reviews of Accelerator Science and Technology*, vol. 1, pp. 185-210, 2008.
- [45] L. Rossi and L. Bottura, "Superconducting magnets for particle accelerators," *Reviews of Accelerator Science and Technology*, vol. 5, pp. 51-89, 2012.
- [46] H. Rogalla and P. H. Kes, *See recollections of A. Greene in B. Strauss and P. Lee, "Nb-Ti - from beginnings to perfection," 100 years of superconductivity*: Taylor & Francis, 2011.
- [47] B. Strauss, R. Remsbottom, P. Reardon, C. Curtis, and W. McDonald, "Results of the Fermilab wire production program," *Magnetics, IEEE Transactions on*, vol. 13, pp. 487-490, 1977.
- [48] D. Larbalestier, K. Hemachalam, P. Lee, W. McDonald, P. O'Larey, R. Scanlan, *et al.*, "High critical current densities in industrial scale composites made from high homogeneity Nb 46. 5 Ti," Applied Superconductivity Center, University of Wisconsin-Madison, Madison, WI1985.
- [49] L. Rossi, A. Szeberenyi, and C. Sutton, "See also: "EU supports the LHC high-luminosity study", CERN Bulletin, Issue No. 45-46/2011; "The light at the end of the tunnel gets brighter", CERN Bulletin, Issue No. 32-34/2014.," CERN Courier, Jan 28, 2013.
- [50] E. Todesco, H. Allain, G. Ambrosio, G. Arduini, F. Cerutti, R. De Maria, *et al.*, "A First Baseline for the Magnets in the High Luminosity LHC Insertion Regions," *Applied Superconductivity, IEEE Transactions on*, vol. 24, pp. 1-5, 2014.
- [51] "The European Strategy for Particle Physics, in "Accelerating Science and Innovation, Societal Benefits of European Research in Particle Physics", produced by the European Particle Physics Communication Network for the CERN Council, May 2013, CERN-Brochure-2013-004-ENG.," in ed.
- [52] J. Osborne and C. Waaijer, "Pre-feasibility study for an 80km tunnel project at CERN," *CERN EDMS*, 2012.
- [53] L. Bottura, G. de Rijk, L. Rossi, and E. Todesco, "Advanced Accelerator Magnets for Upgrading the LHC," *Applied Superconductivity, IEEE Transactions on*, vol. 22, pp. 4002008-4002008, 2012.
- [54] R. Assmann, L. Rossi, F. Zimmermann, O. Dominguez Sanchez, G. de Rijk, J. M. Jimenez, *et al.*, "First thoughts on a higher-energy LHC," 2010.
- [55] A. Apyan, "CEPC-SPPC Preliminary Conceptual Design Report," IHEP-CEPCPP-DR-2015-01, IHEP-AC-2015-012015.
- [56] S. Geer, "Muon colliders and neutrino factories," *arXiv preprint arXiv:1202.2140*, 2012.
- [57] "Muon Colliders and Neutrino Factories", W. Chou Ed., ICFA Beam Dynamics Newsletter No. 55, August 2011.
- [58] A. Kovalenko, "Nuclotron: status & future," in *Proceedings of EPAC*, 2000.
- [59] P. Spiller, U. Blell, H. Eickhoff, E. Floch, E. Fischer, P. Hülsmann, *et al.*, "Status of the Fair SIS100/300 Synchrotron design," in *Particle Accelerator Conference, 2007. PAC. IEEE*, 2007, pp. 1419-1421.
- [60] G. Moritz, J. Kaugerts, J. Escallier, G. Ganetis, A. K. Jain, A. Marone, *et al.*, "Recent Test Results of the Fast-Pulsed 4 T Cos θ Dipole GSI 001," in *Particle Accelerator Conference, 2005. PAC 2005. Proceedings of the*, 2005, pp. 683-685.
- [61] P. Fabbriatore, F. Alessandria, G. Bellomo, S. Farinon, U. Gambardella, J. Kaugerts, *et al.*, "Development of a Curved Fast Ramped Dipole for FAIR SIS300," *Applied Superconductivity, IEEE Transactions on*, vol. 18, pp. 232-235, 2008.
- [62] (2001). *Snowmass T2 Summary Reports of the Snowmass Working Groups*. Available: <http://www.snowmass2001.org>
- [63] S. A. Gourlay, "Post-LHC accelerator magnets," *Applied Superconductivity, IEEE Transactions on*, vol. 12, pp. 67-74, 2002.
- [64] W. Ansorge, J. Billan, K. Henrichsen, H. Laeger, P. Lebrun, R. Perin, *et al.*, "The prototype superconducting quadrupole magnet for the CERN Intersecting Storage Rings," in *Proc. 6th Int. Conf. on Magnet Technology, Bratislava and CERN ISR-BCM/77-52*, 1977.
- [65] D. E. Johnson, "The B \tilde{A} Low-Beta Insertion Design for the Tevatron," *Nuclear Science, IEEE Transactions on*, vol. 32, pp. 1672-1674, 1985.
- [66] K. Koepke, E. Fisk, G. Mulholland, and H. Pfeffer, "The Tevatron BO Low Beta System," *Nuclear Science, IEEE Transactions on*, vol. 32, pp. 1675-1677, 1985.
- [67] D. A. Finley, R. P. Johnson, and F. Willeke, "Control and Initial Operation of the Fermilab BO Low \tilde{A} Insertion," *Nuclear Science, IEEE Transactions on*, vol. 32, pp. 1678-1680, 1985.
- [68] R. Gupta, M. Anerella, G. Ganetis, M. Garber, A. Ghosh, A. Greene, *et al.*, "Large aperture quadrupoles for RHIC interaction regions," in *Particle Accelerator Conference, 1993., Proceedings of the 1993*, 1993, pp. 2745-2747 vol.4.
- [69] J. Schmalzle, M. Anerella, G. Ganetis, A. Ghosh, R. Gupta, A. Jain, *et al.*, "RHIC D0 insertion dipole design iterations during production," in *Particle Accelerator Conference, 1997. Proceedings of the 1997*, 1997, pp. 3356-3358 vol.3.
- [70] G. Morgan, ""Design of the Large Aperture Superconducting Magnet DX," in *Conference on the Computation of the Electromagnetic Fields*, Compumag, Berlin, Germany, 1995.
- [71] O. S. Brüning, P. Collier, P. Lebrun, S. Myers, R. Ostojic, J. Poole, *et al.*, "LHC Design Report," 2004.
- [72] J. Strait, "Very high gradient quadrupoles," in *Particle Accelerator Conference, 2001. PAC 2001. Proceedings of the 2001*, 2001, pp. 176-180 vol.1.

- [73] A. Yamamoto, T. Taylor, K. Tanaka, V. Kovachev, N. Ohuchi, K. Tsuchiya, *et al.*, "Development of a superconducting insertion quadrupole model magnet for the large Hadron collider," SCAN-98030171997.
- [74] A. Yamamoto, T. Nakamoto, T. Ogitsu, N. Ohuchi, Y. Ajima, N. Higashi, *et al.*, "Production and measurement of the MQXA series of LHC low- β insertion quadrupoles," *Applied Superconductivity, IEEE Transactions on*, vol. 15, pp. 1084-1089, 2005.
- [75] Y. Ajima, N. Higashi, M. Iida, N. Kimura, T. Nakamoto, T. Ogitsu, *et al.*, "The MQXA quadrupoles for the LHC low-beta insertions," *Nuclear Instruments and Methods in Physics Research Section A: Accelerators, Spectrometers, Detectors and Associated Equipment*, vol. 550, pp. 499-513, 2005.
- [76] R. Bossert, T. Heger, S. Gourlay, S. Caspi, A. McInturff, R. Scanlan, *et al.*, "Design of a high gradient quadrupole for the LHC interaction regions," in *Conf. Proc.*, 1997, pp. 2270-2272.
- [77] L. Rossi and O. Brüning, "High Luminosity Large Hadron Collider A description for the European Strategy Preparatory Group," 2012.
- [78] F. Borgnolutti, G. Ambrosio, S. I. Bermudez, D. Cheng, D. Dietderich, H. Felice, *et al.*, "Magnetic Design Optimization of a 150 mm Aperture Low-Beta Quadrupole for the HiLumi LHC," *Applied Superconductivity, IEEE Transactions on*, vol. 24, pp. 1-5, 2014.
- [79] S. E. Bartlett, S. Caspi, D. R. Dietderich, P. Ferracin, S. A. Gourlay, C. R. Hannaford, *et al.*, "An R&D approach to the development of long Nb₃Sn accelerator magnets using the key and bladder technology," *Applied Superconductivity, IEEE Transactions on*, vol. 15, pp. 1136-1139, 2005.
- [80] G. Apollinari, "High Field Magnet Development Toward the High Luminosity LHC," 2014.
- [81] T. Nakamoto, M. Sugano, X. Qingjin, H. Kawamata, S. Enomoto, N. Higashi, *et al.*, "Model Magnet Development of D1 Beam Separation Dipole for the HL-LHC Upgrade," *Applied Superconductivity, IEEE Transactions on*, vol. 25, pp. 1-5, 2015.
- [82] A. Zlobin, B. Auchmann, G. Apollinari, E. Barzi, M. Karppinen, V. Kashikhin, *et al.*, "Development of Nb₃Sn 11 T single aperture demonstrator dipole for LHC upgrades," in *Conf. Proc.*, 2011, pp. 1460-1462.
- [83] M. Karppinen, N. Andreev, G. Apollinari, B. Auchmann, E. Barzi, R. Bossert, *et al.*, "Design of 11 T Twin-Aperture Nb₃Sn Dipole Demonstrator Magnet for LHC Upgrades," *Applied Superconductivity, IEEE Transactions on*, vol. 22, pp. 4901504-4901504, 2012.
- [84] A. Zlobin, D. Smekens, A. Nobrega, B. Auchmann, M. Karppinen, I. Novitski, *et al.*, "Status of 11 T 2-in-1 Nb₃Sn Dipole Development for LHC," 2014.
- [85] A. Zlobin, N. Andreev, G. Apollinari, E. Barzi, G. Chlachidze, A. Nobrega, *et al.*, "QUENCH PERFORMANCE OF THE FIRST TWIN-APERTURE 11 T DIPOLE FOR LHC UPGRADES."
- [86] F. Savary, "Status of the 11 T Nb₃Sn Dipole Project for the LHC," *IEEE Trans. Appl. Supercond*, vol. 25, 2015.
- [87] G. Ambrosio, N. Andreev, M. Anerella, E. Barzi, R. Bossert, S. Caspi, *et al.*, "LARP Long Quadrupole Design," *Applied Superconductivity, IEEE Transactions on*, vol. 18, pp. 268-272, 2008.
- [88] . *Future Circular Collider Workshop*. Available: <http://indico.cern.ch/event/340703/page/3>
- [89] K. Oide, "Electron-Positron Circular Colliders," *Reviews of Accelerator Science and Technology*, vol. 7, pp. 35-48, 2014.
- [90] T. Taylor, "Technological aspects of the LEP low-beta insertions," *Nuclear Science, IEEE Transactions on*, vol. 32, pp. 3704-3706, 1985.
- [91] P. Lebrun, S. Pichler, T. Taylor, T. Tortschanoff, and L. Walckiers, "Design, test and performance of the prototype superconducting quadrupole for the LEP low-beta insertions," *Magnetics, IEEE Transactions on*, vol. 24, pp. 1361-1364, 1988.
- [92] J. Billan, K. Henrichsen, H. Laeger, P. Lebrun, R. Perin, S. Pichler, *et al.*, "The eight superconducting quadrupoles for the ISR high-luminosity insertion," in *11th International Conference on High-Energy Accelerators*, 1980, pp. 848-852.
- [93] T. Taylor, T. Tortschanoff, G. Trinquart, and L. Williams, "Design of the Superconducting Quadrupoles for the LEP200 Low-beta Insertions," *Magnetics, IEEE Transactions on*, vol. 28, pp. 382-385, 1992.
- [94] J. J. Welch, G. E. Dugan, E. Nordberg, and D. Rice, "The superconducting interaction region magnet system for the CESR phase III upgrade," in *Particle Accelerator Conference, 1997. Proceedings of the 1997*, 1997, pp. 3383-3385 vol.3.
- [95] S. Henderson, J. Welch, M. Billing, G. Cherwinka, G. Codner, G. Dugan, *et al.*, "CESR Phase III interaction region," in *Particle Accelerator Conference, 1999. Proceedings of the 1999*, 1999, pp. 3221-3223.
- [96] M. Begg, T. Taylor, and A. Ijspeert, "Construction and test of SC quadrupoles for the LEP200 low beta insertions," CERN-LEP2-Note-94-141994.
- [97] Y. Wu, C. Yu, F. Chen, J. Pang, J. Zhang, M. Wang, *et al.*, "The magnet system of the BEPCII interaction region," *Applied Superconductivity, IEEE Transactions on*, vol. 20, pp. 360-363, 2010.
- [98] B. Parker and J. Escallier, "Serpentine Coil Topology for BNL Direct Wind Superconducting Magnets," in *Particle Accelerator Conference, 2005. PAC 2005. Proceedings of the*, 2005, pp. 737-739.
- [99] K. Kanazawa, H. Nakayama, T. Ogitsu, N. Ohuchi, T. Ozaki, K. Satoh, *et al.*, "The interaction region of KEKB," *Nuclear Instruments and Methods in Physics Research Section A: Accelerators, Spectrometers, Detectors and Associated Equipment*, vol. 499, pp. 75-99, 2003.
- [100] M. Masuzawa. (2010). *Next Generation B-factories*. Available: <http://www.jacow.org/>
- [101] P. Raimondi. (2006). *Introduction to Super B-Accelerator*. Available: <http://www.Inf.infn.it/conference/superb06/prog.html>
- [102] N. Ohuchi, Y. Arimoto, N. Higashi, H. Koiso, A. Morita, Y. Ohnishi, *et al.*, "Design of the

- superconducting magnet system for the SuperKEKB interaction region," *Proceedings of NA-PAC, Pasadena, California*, 2013.
- [103] B. Parker, M. Anerella, J. Escallier, A. Ghosh, H. Hocker, A. Jain, *et al.*, "Superconducting corrector IR magnet production for SuperKEKB," *THPBA07, NA-PAC*, vol. 1, 2013.
- [104] . *Belle II Technical Design Report*. Available: <http://xxx.lanl.gov/abs/1011.0352>
- [105] N. Ohuchi, Y. Arimoto, N. Higashi, M. Iwasaki, M. Kawai, Y. Kondou, *et al.*, "Design and Construction of the SuperKEKB QC1 Final Focus Superconducting Magnets," *Applied Superconductivity, IEEE Transactions on*, vol. 25, pp. 1-4, 2015.
- [106] . *International Linear Collider Technical Design Report*. Available: <http://www.linearcollider.org/ILC/Publications/Technical-Design-Report>
- [107] V. Kashikhin, N. Andreev, Y. Orlov, D. Orris, and M. Tartaglia, "Superconducting magnets for SCRF cryomodules at front end of linear accelerators," *Proceedings of IPAC*, vol. 10, pp. 379-381, 2010.
- [108] V. Kashikhin, N. Andreev, J. Kerby, Y. Orlov, N. Solyak, M. Tartaglia, *et al.*, "Superconducting splittable quadrupole magnet for linear accelerators," *Applied Superconductivity, IEEE Transactions on*, vol. 22, pp. 4002904-4002904, 2012.
- [109] N. Kimura, N. Andreev, V. Kashikhin, J. Kerby, M. Takahashi, M. Tartaglia, *et al.*, "Cryogenic performance of a conduction-cooling splittable quadrupole magnet for ILC cryomodules," in *ADVANCES IN CRYOGENIC ENGINEERING: Transactions of the Cryogenic Engineering Conference-CEC*, 2014, pp. 407-415.
- [110] N. Andreev, V. S. Kashikhin, J. Kerby, N. Kimura, M. Takahashi, M. A. Tartaglia, *et al.*, "Conduction Cooling Test of a Splittable Quadrupole for ILC Cryomodules," *Applied Superconductivity, IEEE Transactions on*, vol. 23, pp. 3500305-3500305, 2013.
- [111] A. Seryi, J. Amann, R. Arnold, F. Asiri, K. Bane, P. Bellomo, *et al.*, "Design of the beam delivery system for the international linear collider," in *Particle Accelerator Conference, 2007. PAC. IEEE*, 2007, pp. 1985-1987.
- [112] B. Parker, M. Anerella, J. Escallier, P. He, A. Jain, A. Marone, *et al.*, "The superconducting magnets of the ILC beam delivery system," in *Particle Accelerator Conference, 2007. PAC. IEEE*, 2007, pp. 3196-3198.
- [113] B. Parker, M. Anerella, J. Escallier, A. Ghosh, A. Jain, A. Marone, *et al.*, "BNL Direct Wind superconducting magnets," *Applied Superconductivity, IEEE Transactions on*, vol. 22, pp. 4101604-4101604, 2012.
- [114] A. Drozhdin, M. Lopes, N. Mokhov, A. Seryi, A. Zlobin, V. Kashikhin, *et al.*, "Radiation and thermal analysis of superconducting quadrupoles in the interaction region of linear collider," in *Conf. Proc.*, 2008, p. WEPD036.
- [115] A. Zlobin, Y. Alexahin, V. Kashikhin, and N. Mokhov, "Magnet designs for muon collider ring and interactions regions," *arXiv preprint arXiv:1202.0270*, 2012.
- [116] I. Novitski, V. V. Kashikhin, N. Mokhov, and A. V. Zlobin, "Conceptual Designs of Dipole Magnet for Muon Collider Storage Ring," *Applied Superconductivity, IEEE Transactions on*, vol. 21, pp. 1825-1828, 2011.
- [117] V. Kashikhin, Y. Alexahin, N. Mokhov, and A. Zlobin, "High-Field Combined-Function Magnets for a 1.5×1.5 TeV Muon Collider Storage Ring," *THPPD036, these proceedings*, 2012.
- [118] Y. Alexahin, E. Gianfelice-Wendt, V. Kashikhin, N. Mokhov, A. Zlobin, and V. Alexakhin, "Muon collider interaction region design," *Physical Review Special Topics-Accelerators And Beams*, vol. 14, p. 061001, 2011.
- [119] V. Kashikhin, Y. Alexahin, N. Mokhov, and A. Zlobin, "Magnets for Interaction Regions of a 1.5×1.5 TeV Muon Collider," *THPPD035, these proceedings*, 2012.
- [120] Y. Hayato and T. K. collaboration, "T2K at J-PARC," *Nuclear Physics B-Proceedings Supplements*, vol. 143, pp. 269-276, 2005.
- [121] T. Ogitsu, Y. Makida, T. Kobayashi, Y. Ajima, Y. Doi, N. Higashi, *et al.*, "Superconducting magnet system at the 50 GeV proton beam line for the J-PARC neutrino experiment," *Applied Superconductivity, IEEE Transactions on*, vol. 14, pp. 604-607, 2004.
- [122] T. Ogitsu, Y. Ajima, M. Anerella, J. Escallier, G. Ganetis, R. Gupta, *et al.*, "Superconducting combined function magnet system for J-PARC neutrino experiment," *Applied Superconductivity, IEEE Transactions on*, vol. 15, pp. 1175-1180, 2005.
- [123] K. I. Sasaki, T. Nakamoto, N. Kimura, T. Tomaru, T. Ogitsu, N. Higashi, *et al.*, "Test Results of Superconducting Combined Function Magnets for the J-PARC Neutrino Beam Line," *Applied Superconductivity, IEEE Transactions on*, vol. 17, pp. 1083-1086, 2007.
- [124] T. Ogitsu, Y. Ajima, O. Araoka, Y. Fujii, N. Hasting, N. Higashi, *et al.*, "Operation of superconducting combined function magnet system for J-PARC neutrino beam line," *Proceedings of IPAC 2010, MOPEB033*, 2010.
- [125] T. Ogitsu, Y. Makida, T. Nakamoto, K. Sasaki, O. Araoka, Y. Fujii, *et al.*, "Status of Superconducting Magnet System for J-PARC Neutrino Beam Line," *Applied Superconductivity, IEEE Transactions on*, vol. 23, pp. 4001506-4001506, 2013.
- [126] G. Bennett, B. Bousquet, H. Brown, G. Bunce, R. Carey, P. Cushman, *et al.*, "Measurement of the negative muon anomalous magnetic moment to 0.7 ppm," *Physical review letters*, vol. 92, p. 161802, 2004.
- [127] G. Danby, L. Addressi, Z. Armoza, J. Benante, H. Brown, G. Bunce, *et al.*, "The Brookhaven muon storage ring magnet," *Nuclear Instruments and Methods in Physics Research Section A: Accelerators, Spectrometers, Detectors and Associated Equipment*, vol. 457, pp. 151-174, 2001.
- [128] A. Yamamoto and Y. Makida, "Advances in superconducting magnets for high energy and

- astroparticle physics," *Nuclear Instruments and Methods in Physics Research Section A: Accelerators, Spectrometers, Detectors and Associated Equipment*, vol. 494, pp. 255-265, 2002.
- [129] F. Krienen, G. T. Danby, W. Meng, C. Pai, W. B. Sampson, K. A. Woodle, *et al.*, "The superconducting inflector dipole for the muon g-2 storage ring," *Applied Superconductivity, IEEE Transactions on*, vol. 5, pp. 671-674, 1995.
- [130] A. Yamamoto, Y. Makida, K. Tanaka, F. Krienen, B. Roberts, H. Brown, *et al.*, "The superconducting inflector for the BNL g-2 experiment," *Nuclear Instruments and Methods in Physics Research Section A: Accelerators, Spectrometers, Detectors and Associated Equipment*, vol. 491, pp. 23-40, 2002.
- [131] I. Itoh, T. Sasaki, S. Minamino, and T. Shimizu, "Magnetic shielding properties of NbTi/Nb/Cu multilayer composite tubes," *Applied Superconductivity, IEEE Transactions on*, vol. 3, pp. 177-180, 1993.
- [132] . *Fermilab Muon g-2 Experiment*. Available: <http://muon-g-2.fnal.gov/>
- [133] T. Ogitsu, "Progress and Prospect of Superconducting Magnet Systems in J-PARC," *Applied Superconductivity, IEEE Transactions on*, vol. 21, pp. 1742-1747, 2011.
- [134] N. Saito, "A novel precision measurement of muon g-2 and EDM at J-PARC," in *GUT2012*, 2012, pp. 45-56.
- [135] K. I. Sasaki, H. Iinuma, N. Kimura, T. Ogitsu, A. Yamamoto, H. Nakayama, *et al.*, "Study on Field Measurement and Ground Vibration for Superconducting Solenoid of New g-2 Experiment at J-PARC," *Applied Superconductivity, IEEE Transactions on*, vol. 21, pp. 1748-1751, 2011.
- [136] E. Willen, R. Gupta, A. Jain, E. Kelly, G. Morgan, J. Muratore, *et al.*, "A helical magnet design for RHIC," in *Particle Accelerator Conference, 1997. Proceedings of the 1997*, 1997, pp. 3362-3364 vol.3.
- [137] E. Willen, E. Kelly, M. Anerella, J. Escallier, G. Ganetis, A. Ghosh, *et al.*, "Construction of helical magnets for RHIC," in *Particle Accelerator Conference, 1999. Proceedings of the 1999*, 1999, pp. 3161-3163 vol.5.
- [138] R. D. Schlueter, "Wiggler and undulator insertion devices," *LBL Report-35565*, May, 1994.
- [139] H. Nishimura and D. Robin, "Impact of superbends at the ALS," in *Particle Accelerator Conference, 1999. Proceedings of the 1999*, 1999, pp. 203-205 vol.1.
- [140] A. Artamonov, L. Barkov, V. Baryshev, N. Bashtovoy, N. Vinokurov, E. Gluskin, *et al.*, "First results of the work with a superconducting "snake" at the VEPP-3 storage ring," *Nuclear Instruments and Methods*, vol. 177, pp. 239-246, 1980.
- [141] C. Bazin, M. Billardon, D. Deacon, Y. Farge, J. Ortega, J. Perot, *et al.*, "First results of a superconducting undulator on the ACO storage ring," *Journal de Physique Lettres*, vol. 41, pp. 547-550, 1980.
- [142] P. Emma, N. Holtkamp, H. Nuhn, D. Arbelaez, J. Corlett, S. Myers, *et al.*, "A plan for the development of superconducting undulator prototypes for LCLS-II and future FELs," in *FEL 2014 Conference Proceedings, Basel, Switzerland*, 2014.
- [143] R. Schlueter, S. Marks, S. Prestemon, and D. Dietderich, "Superconducting undulator research at LBNL," 2004.
- [144] S. Prestemon and R. Schlueter, "Undulator options for soft X-ray free electron lasers," in *31st International FEL Conference, Liverpool*, 2009.
- [145] S. Prestemon, D. Dietderich, A. Madur, S. Marks, and R. Schlueter, "High performance short-period undulators using high temperature superconductor tapes," in *PAC proceedings*, 2009, pp. 1-3.
- [146] K. Noda, T. Furukawa, Y. Hara, T. Inaniwa, Y. Iwata, K. Katagiri, *et al.*, "Recent progress and future plan of heavy-ion radiotherapy facility, HIMAC," *Nucl Instrum Meth*, vol. 281, 2010.
- [147] Y. Iwata, K. Noda, T. Murakami, T. Shirai, T. Furukawa, T. Fujita, *et al.*, "Development of a compact superconducting rotating-gantry for heavy-ion therapy," *Journal of radiation research*, vol. 55, pp. i24-i25, 2014.
- [148] J. R. Alonso and T. A. Antaya, "Superconductivity in medicine," *Reviews of Accelerator Science and Technology*, vol. 5, pp. 227-263, 2012.
- [149] S. Suzuki, Y. Iwata, K. Noda, T. Shirai, T. Furukawa, T. Fujita, *et al.*, "MAGNETIC-FIELD MEASUREMENTS OF SUPERCONDUCTING MAGNETS FOR A HEAVY-ION ROTATING-GANTRY AND BEAM-TRACKING SIMULATIONS," 1994.
- [150] D. I. Meyer and R. Flasck, "A new configuration for a dipole magnet for use in high energy physics applications," *Nuclear Instruments and Methods*, vol. 80, pp. 339-341, 4/15/ 1970.
- [151] D. S. Robin, D. Arbelaez, S. Caspi, C. Sun, A. Sessler, W. Wan, *et al.*, "Superconducting toroidal combined-function magnet for a compact ion beam cancer therapy gantry," *Nuclear Instruments and Methods in Physics Research Section A: Accelerators, Spectrometers, Detectors and Associated Equipment*, vol. 659, pp. 484-493, 12/11/ 2011.
- [152] C. L. Goodzeit, M. J. Ball, and R. B. Meinke, "The double-helix dipole - a novel approach to accelerator magnet design," *Applied Superconductivity, IEEE Transactions on*, vol. 13, pp. 1365-1368, 2003.
- [153] A. V. Gavrilin, M. D. Bird, V. E. Keilin, and A. V. Dudarev, "New concepts in transverse field magnet design," *Applied Superconductivity, IEEE Transactions on*, vol. 13, pp. 1213-1216, 2003.
- [154] A. Devred, B. Baudouy, D. Baynham, T. Boutboul, S. Canfer, M. Chorowski, *et al.*, "Overview and status of the next European dipole joint research activity," *Superconductor Science and Technology*, vol. 19, p. S67, 2006.
- [155] C. Goodzeit, R. Meinke, and M. Ball, "Combined function magnets using double-helix coils," in *Particle Accelerator Conference, 2007. PAC. IEEE*, 2007, pp. 560-562.
- [156] S. Caspi, D. Dietderich, P. Ferracin, N. Finney, M. Fuery, S. Gourlay, *et al.*, "Design, fabrication, and test

- of a superconducting dipole magnet based on tilted solenoids," *Applied Superconductivity, IEEE Transactions on*, vol. 17, pp. 2266-2269, 2007.
- [157] H. Witte, T. Yokoi, S. L. Sheehy, K. Peach, S. Pattalwar, T. Jones, *et al.*, "The advantages and challenges of helical coils for small accelerators—A case study," *Applied Superconductivity, IEEE Transactions on*, vol. 22, pp. 4100110-4100110, 2012.
- [158] S. Caspi, D. Arbelaez, L. Brouwer, D. Dietderich, H. Felice, R. Hafalia, *et al.*, "A superconducting magnet mandrel with minimum symmetry laminations for proton therapy," *Nuclear Instruments and Methods in Physics Research Section A: Accelerators, Spectrometers, Detectors and Associated Equipment*, vol. 719, pp. 44-49, 2013.
- [159] R. Geller, F. Bourg, P. Briand, J. Debernardi, M. Delaunay, B. Jacquot, *et al.*, "The Grenoble ECRIS status 1987 and proposal for ECRIS scaling," in *International Conference on ECR Ion Sources and their Applications, NSCL Report# MSU CP-47, Michigan, S*, 1987.
- [160] L. Sun, "High Intensity Operation for Heavy Ion Cyclotron of Highly Charged ECR Ion Sources."
- [161] D. Leitner, C. Lyneis, D. Collins, R. Dwinell, M. Galloway, and D. Todd, "First results for the 28 GHZ operation of the superconducting ECR ion source VENUS," 2005.
- [162] G. Machicoane, M. Doleans, O. Kester, E. Pozdeyev, T. Ropponen, L. Sun, *et al.*, "ECR Ion Sources For The Facility For Rare Isotope Beams (FRIB) Project At Michigan State University"," *ECRIS*, vol. 10, p. 14, 2012.
- [163] C. Lyneis, P. Ferracin, S. Caspi, A. Hodgkinson, and G. Sabbi, "Concept for a fourth generation electron cyclotron resonance ion sourcea)," *Review of Scientific Instruments*, vol. 83, p. 02A301, 2012.
- [164] L. Sun, W. Lu, Y. Feng, W. Zhang, X. Zhang, Y. Cao, *et al.*, "Progress of superconducting electron cyclotron resonance ion sources at Institute of Modern Physics (IMP) a)," *Review of Scientific Instruments*, vol. 85, p. 02A942, 2014.
- [165] H. R. A. Detector, N. Walls, N. E. R. Observer, L. E. Beam, I. Trap, and R. F. Separator, "National Superconducting Cyclotron Laboratory."
- [166] A. Zeller, J. DeKamp, C. Magsig, J. Wagner, and D. Pendell, "Superconducting beamline elements for the NSCL spectrograph," *Applied Superconductivity, IEEE Transactions on*, vol. 5, pp. 1032-1035, 1995.
- [167] H. Sato, T. Kubo, Y. Yano, K. Kusaka, J.-i. Ohnishi, K. Yoneda, *et al.*, "Superconducting Dipole Magnet for SAMURAI Spectrometer," *Applied Superconductivity, IEEE Transactions on*, vol. 23, pp. 4500308-4500308, 2013.
- [168] G. e. al. (2008). *Technical Design Report on the Super-FRS* Available: <http://repository.gsi.de/record/54552/files/GSI-2013-05264.pdf>
- [169] H. Müller, H. Leibrock, M. Winkler, P. Schnizer, and E. Fischer, "Status of the Super-FRS Magnet Development for FAIR," *Proceedings of IPAC2013, Shanghai, China*, pp. 3519-3521, 2013.
- [170] H. Leibrock, E. Floch, G. Moritz, L. Ma, W. Wu, P. Yuan, *et al.*, "Prototype of the Superferric Dipoles for the Super-FRS of the FAIR-Project," *Applied Superconductivity, IEEE Transactions on*, vol. 20, pp. 188-191, 2010.
- [171] F. Borgnolutti, B. Auchmann, L. Bottura, F. Carra, G. Foffano, J. Gomes De Faria, *et al.*, "Construction of the CERN fast cycled superconducting dipole magnet prototype," *Applied Superconductivity, IEEE Transactions on*, vol. 22, pp. 4001604-4001604, 2012.
- [172] H. Khodzhbagiyani, P. Akishin, A. Bychkov, A. Donyagin, A. Galimov, O. Kozlov, *et al.*, "Status of the design and test of superconducting magnets for the NICA project," *RuPAC2012, St. Petersburg*, 2012.
- [173] H. Piekarz, J. Blowers, S. Hays, and V. Shiltsev, "Design, Construction, and Test Arrangement of a Fast-Cycling HTS Accelerator Magnet," *Applied Superconductivity, IEEE Transactions on*, vol. 24, pp. 1-4, 2014.
- [174] J. C. Colvin, H. Hinterberger, F. R. Huson, W. W. Mackay, T. L. Mann, P. M. McIntyre, *et al.*, "The high field superferric magnet: Design and test of a new dipole magnet for future hadron colliders," *Nuclear Instruments and Methods in Physics Research Section A: Accelerators, Spectrometers, Detectors and Associated Equipment*, vol. 270, pp. 207-211, 1988.
- [175] G. W. Foster and V. Kashikhin, "Superconducting superferric dipole magnet with cold iron core for the VLHC," *Applied Superconductivity, IEEE Transactions on*, vol. 12, pp. 111-115, 2002.
- [176] A. Milanese, L. Rossi, and H. Piekarz, "Concept of a Hybrid (Normal and Superconducting) Bending Magnet based on Iron Magnetization for 80-100km Lepton/Hadron Colliders," 2014.